

*Report entitled*

---

**Introduction to the Applications of Remote Sensing Techniques on the Tree Health  
Monitoring**

---

By

Project Investigators:

Sr Dr. WONG Man Sing, Charles

Sr Dr. TANG Hon Wai, Conrad

Sr Dr. LAM Lik Shan Lesly

Research Associates:

Mr. CHENG Ho-hang

Miss HUNG Ka-yi

Miss KWOK Yin-tung, Coco

Mr. TANG Tin-hang, Carlos

October 2020

## ABSTRACT

The extreme weather has resulted in potential incidents of tree collapse in recent years. With the public safety and maintenance concerns regarding tree hazards, tree health monitoring is essential to the hyper-dense urban areas in Hong Kong. Different techniques have been applied to detect the problematic trees and to monitor the tree's health condition. Remote Sensing technique is one of effective and efficient approaches utilized in extensive tree health monitoring. This project aims to introduce three Remote Sensing techniques, including thermal infrared imaging, hyperspectral imaging, and multispectral aerial imaging, on the application of tree health monitoring. Accordingly, this project aims to introduce three Remote Sensing techniques, including thermal infrared imaging, hyperspectral imaging, and multispectral aerial imaging, on the application of tree health monitoring. The primary objectives of this project are: (i) to briefly explain the basic principle of the Remote Sensing techniques applying in the tree health monitoring; (ii) to illustrate the overall methodology of monitoring the tree health condition using the Remote Sensing techniques; and (iii) to compare the effectiveness of three Remote Sensing techniques on the tree health detection generally.

The report starts by introducing thermal infrared imaging. By using the thermal camera, tree trunks were observed. Two healthy and two unhealthy trees were selected for illustration. Besides, the image processing and tree trunk extraction were discussed. The following results of each healthy and unhealthy tree's thermal image would be presented with their thermal characteristics. The hyperspectral imaging was used to observe the healthiness of tree canopy. The spectral reflectance of the tree canopy was captured using the handheld hyperspectral camera to evaluate the tree health conditions. In addition, the multispectral reflectance from the tree canopy was used to analyze tree health based on the multispectral aerial images obtained from the Lands Department of Hong Kong SAR. Vegetation indices are the significant tool to examine the tree health status and the Normalized Differencing Vegetation Index (NDVI) with threshold condition was adopted. Since the hyperspectral imaging and multispectral imaging can monitor tree canopy, the consistency of tree health detection from Remote Sensing techniques can be assessed and the relationship of health condition between the tree trunk and tree canopy would be discussed in this study. According to the demonstrated samples, the tree with an unhealthy tree trunk could have a healthy tree canopy and this indicates that there is no absolute relationship between the health status of tree trunk and tree canopy. With the aid of different Remote Sensing techniques, the tree health condition can be detected and identified, and the risk of a particular tree can be assessed through continuous and efficient monitoring.

# TABLE OF CONTENTS

<b>Abstract.....</b>	<b>i</b>
<b>Table of Contents .....</b>	<b>ii</b>
<b>List of Equations .....</b>	<b>vi</b>
<b>List of Figures.....</b>	<b>vii</b>
<b>List of Tables.....</b>	<b>ix</b>
<b>List of Abbreviations.....</b>	<b>x</b>
<b>Chapter 1 INTRODUCTION.....</b>	<b>1</b>
1.1 Background of the Project .....	1
1.2 Main Objectives .....	2
1.3 Project Methodology and Framework .....	3
1.4 Structure of Project and Report.....	5
<b>Chapter 2 LITERATURE REVIEW.....</b>	<b>6</b>
2.1 Basic Concepts of Unhealthy Tree.....	6
2.1.1 Types of Tree Diseases .....	6
2.1.2 Common Symptoms of Sick Tree.....	8
2.2 Thermal Infrared Imaging.....	9
2.2.1 Thermography and Infrared Light .....	9
2.2.2 Principal of Thermal Infrared Camera.....	9
2.2.3 Interpretation of Tree Health Condition under Temperature Differences....	10
2.3 Hyperspectral Imaging (HSI).....	11
2.3.1 Basis of Hyperspectral Remote Sensing.....	11
2.3.2 Sensor Resolution .....	11
2.3.3 Vegetation Studies Under Hyperspectral Data .....	12
2.4 Multispectral Aerial Imaging .....	13
2.4.1 Basis of Multispectral Remote Sensing.....	13
2.4.2 Introduction to Vegetation Index .....	13
<b>Chapter 3 TREE HEALTH MONITORING THROUGH THERMAL INFRARED IMAGING ...</b>	<b>14</b>
3.1 Introduction.....	14
3.2 Study Area.....	16
3.3 Overview of Data and Equipment.....	16
3.4 Methodology .....	18
3.4.1 Data Acquisition .....	18

3.4.1.1	Target Tree Selection .....	18
3.4.1.2	Field Observation.....	20
3.4.2	Data Pre-processing .....	20
3.4.2.1	Data Format Conversion.....	20
3.4.2.2	Tree Trunk Extraction .....	20
3.4.3	Data Interpretation and Analysis .....	22
3.5	Result and Analysis.....	22
3.5.1	Characteristics of Healthy Tree in Thermal Infrared Image .....	22
3.5.2	Characteristics of Unhealthy Tree in Thermal Infrared Image .....	24
3.6	Chapter Summary .....	26

**Chapter 4 TREE HEALTH MONITORING THROUGH HYPERSPECTRAL IMAGING..... 27**

4.1	Introduction.....	27
4.2	Study Area.....	27
4.3	Overview of Data and Equipment.....	28
4.4	Methodology .....	29
4.4.1	Data Acquisition .....	29
4.4.1.1	Target Tree Selection .....	30
4.4.1.2	Field Observation.....	31
4.4.2	Data Pre-processing .....	32
4.4.2.1	Identification of Area of Vegetation.....	32
4.4.3	Healthy Tree Crown Detection .....	34
4.4.3.1	Index for Thresholding of Healthy Leaves .....	35
4.5	Result and Analysis.....	38
4.6	Chapter Summary .....	39

**Chapter 5 TREE HEALTH MONITORING BY MULTISPECTRAL AERIAL IMAGING..... 40**

5.1	Introduction.....	40
5.2	Study Area.....	41
5.3	Overview of Data .....	41
5.4	Methodology .....	42
5.4.1	Identification of Area of Vegetation.....	42
5.4.1.1	Index for Vegetation Extraction .....	43
5.4.1.2	Thresholding .....	44
5.4.2	Healthy Tree Crown Detection .....	46
5.4.2.1	Index for Thresholding of Healthy Leaves .....	47
5.5	Result and Analysis.....	48
5.5.1	Classification of Tree Health Status .....	48
5.6	Chapter Summary .....	53

<b>Chapter 6</b>	<b>TREE HEALTH DETECTION THROUGH COMBINING THREE METHODS .....</b>	<b>54</b>
6.1	Relationship of Health Condition between Tree Trunk and Tree Canopy .....	54
6.2	Result Consistency of the Health Condition of Tree Canopy Detected through Hyperspectral and Multispectral Imaging.....	55
<b>Chapter 7</b>	<b>DISCUSSION AND RECOMMENDATION .....</b>	<b>57</b>
<b>Chapter 8</b>	<b>CONCLUSION .....</b>	<b>59</b>
	<b>REFERENCES.....</b>	<b>60</b>

## LIST OF EQUATIONS

Equation (a). Modified Red Edge Normalized Difference Vegetation Index ( $mNDVI_{750}$ ) .....	33
Equation (b). Carotenoid Reflectance Index 2 ( $CRI_2$ ) .....	35
Equation (c). Anthocyanin Reflectance Index 1 ( $ARI_1$ ) .....	35
Equation (d). Plant Senescence Reflectance Index (PSRI).....	36
Equation (e). Normalized Difference Vegetation Index (NDVI).....	43

## LIST OF FIGURES

Figure 1.1. The framework of the methodology of this project.....	4
Figure 2.1. Leaves attacked by Anthracnose (cited from the University of Arkansas, 2020) .....	7
Figure 2.2. Diffuse cankers (Left) and Spot cankers (Right) (cited from the University of Arkansas, 2020)...	7
Figure 2.3. Logging damage (cited from USDA Forest Service, 2018) .....	8
Figure 2.4. Schematic representation of a generic thermographic measurement (cited from Vidal & Pitarma, 2019) .....	10
Figure 3.1. Location of Victoria Park and Cotton Path.....	16
Figure 3.2. FLIR T650sc (FLIR, 2020) .....	17
Figure 3.3. The overall workflow of this section.....	18
Figure 3.4. Location of the selected trees .....	19
Figure 3.5. Result of tree trunk extraction .....	21
Figure 3.6. IRT of LCSD/WC/00033 (Left) and LCSD_WC_00023 (Right) .....	23
Figure 3.7. IRT of LCSD/WC/00042 (Left) and Tree in Cotton Path (Right).....	25
Figure 3.8. IRT of LCSD/WC/00042 (Left) and Tree in Cotton Path (Right).....	26
Figure 4.1. Boundary of the study area.....	28
Figure 4.2. Specim IQ (SPECIM, SPECTRAL IMAGING LTD, 2020).....	28
Figure 4.3. Overall workflow of this study.....	29
Figure 4.4. Location of the selected trees .....	30
Figure 4.5. RGB of the four sample trees .....	32
Figure 4.6. Result of tree crown extraction.....	34
Figure 4.7. Decision tree of tree health condition classification.....	37
Figure 4.8. Result of tree health condition classification.....	38
Figure 5.1. Spatial extent of the DAP .....	41
Figure 5.2. Overall workflow of this study.....	42
Figure 5.3. Original DAP (Left); False colour composites (Middle); NDVI (Right).....	43
Figure 5.4. NDVI threshold value larger than 0.27 (Sparse and dense vegetation class).....	44
Figure 5.5. Non-vegetation land covers with NDVI > 0.27.....	45
Figure 5.6. Optimized result of thresholding (Left) and NDVI of the delimited area of tree crown (Right) .....	46
Figure 5.7. Difference of reflectance between the healthy and unhealthy vegetation (Stoyanova, Kandilarov, Koutev, Nitcheva, & Dobрева, 2018) .....	47
Figure 5.8. Basic classification of tree health condition.....	48
Figure 5.9. Location of the example of the tree with the significant large ratio of unhealthy tree crown.....	49
Figure 5.10. Tree health mapping of the study area.....	50
Figure 5.11. Tree health mapping of the roadside.....	51
Figure 5.12. Location of the six sample trees and their detailed health condition .....	51
Figure 6.1. Health condition of tree trunk and tree canopy of the 4 sample trees .....	54
Figure 6.2. Health condition of tree canopy of the 4 sample trees from hyperspectral imaging and multispectral imaging .....	56

## LIST OF TABLES

Table 3.1. Metadata of the IRT acquired by FLIR T650sc .....	17
Table 3.2. Properties of the selected tree .....	19
Table 3.3. Quantitative presentation of characteristic of the selected healthy tree .....	23
Table 3.4. Quantitative presentation of characteristic of the selected unhealthy tree .....	25
Table 4.1. Metadata of the Specim Dataset acquired by Specim IQ.....	29
Table 4.2. Summary of VIs' equation and their threshold .....	36
Table 4.3. Quantitative presentation of the tree health condition of the four sample trees.....	39
Table 5.1. Metadata of the DAP.....	42
Table 5.2. Quantitative presentation of the tree health condition of the six sample trees .....	52

## LIST OF ABBREVIATIONS

AOI	Area of Interest
ARI <sub>1</sub>	Anthocyanin Reflectance Index 1
CRI <sub>2</sub>	Carotenoid Reflectance Index 2
DAP	Digital Aerial Photo
HSI	Hyperspectral Imaging
IRT	Infrared Thermography
mNDVI <sub>750</sub>	Modified Red Edge Normalized Difference Vegetation Index
NDVI	Normalized Difference Vegetation Index
NIR	Near-Infrared
OVT	Old and Valuable Tree
PSRI	Plant Senescence Reflectance Index
SMO	Survey and Mapping Office
ST	Sample Tree
SWIR	Short-Wave Infrared
UHI	Urban Heat Island
VI	Vegetation Index

## CHAPTER 1 INTRODUCTION

---

### 1.1 Background of the Project

Trees play the most essential role in land-atmosphere interactions and cycles of the earth systems. Based on the North Carolina Climate Office (2020), trees play a crucial part in the water cycle. Besides, vegetation balances the level of carbon dioxide of the earth through the process of photosynthesis. Basically, the trees could reduce the amount of carbon emitted from human activities, such as power plants, traffic, industrial activities etc. through absorbing the carbon dioxide, and oxygen is released concurrently (Nowak, 1994). Apart from ecological value, the trees also promote public mental health and living quality. Under landscape design or even urban foresting, the Urban Heat Island (UHI) effect and air pollution can be mitigated. Trees greatly benefit the people living around them by positively benefiting mental health and well-being, reducing stress, and encouraging outdoor exercise. In addition to the ecosystem benefits, they could receive improved environmental quality and improved amenity, which comes with planted areas (Shanahan et al., 2015).

In view of preserving the tree's benefits, tree maintenance is continuously implementing in Hong Kong. It is reported that the tree risk assessment is carried out mainly in two stages composed of area basis and tree basis assessment. Through these assessments, the relevant departments will have brief information on the trees with an obvious health problem or structural problem located in places with high pedestrian or traffic flow, and thereafter followed with a visual inspection of the trees under systematic methods. For instance, during the tree inspections, it is necessary to identify whether there is a defect inside the tree, such as decay or tree cavity, with the aid of resistograph or sonic tomography. Nevertheless, tree health monitoring highly relies on a visual inspection conducted by the Certified Arborist. Although tree health inspections can acquire the information regarding the trees' health condition as well as the structure, this process is time- and labour-dependent. Accordingly, relying on the trees' visual inspection under systematic methods may not be efficient for continuously monitor a significant number of trees in Hong Kong.

Moreover, over the past few years, tree collapse accidents arouse public attention to the risk from the trees. Especially at the end of August 2018, Hong Kong had been suffering from one of the most powerful typhoons -- Mangkhut. It caused more than 60,800 trees to collapse and result in human casualty and property loss (Hong Kong Observatory, 2018). In view of this, several organizations commenced the study and have been developing state-of-the-art technology for tree health monitoring. In accordance with the research commenced by The Hong Kong Polytechnic University (2018), Dr. Charles Wong, Associate Professor of the Department of Land Surveying and Geo-Informatics, has established an intelligent system, named Smart Tree Monitoring System for Urban Tree Management, to monitor the tilt angle and root displacement of trees, issue early warnings, and conduct in-depth research on various factors that affect trees' stability. In response to monitoring the stability of the tree, the project team installed smart sensors at the bottom of the tree trunks to monitor the tilt angles.

Aside from the smart sensor, Remote Sensing techniques become increasingly common in tree health monitoring. Tree health monitoring employs the spectral response reflected from the trees and turns it into the classified cluster, generally healthy and unhealthy group, based on the divergence of the spectral reflectance of different bands (Xiao & McPherson, 2005). In reference to several studies of tree health monitoring, Remote Sensing techniques have been utilized. Typically, infrared thermography, hyperspectral imaging, and multispectral aerial imaging can remotely obtain the data of the tree health status (Calderón, Navas-Cortés, Lucena, & Zarco-Tejada, 2013). Compared with the traditional visual inspection methods Remote Sensing techniques can detect the problem of the tree in a non-invasive manner and enable distant and contactless investigation of the tree. According to Lévesque and King (2003), hyperspectral and multispectral imaging can provide enhanced details concerning the tree health condition from the tree canopy. As such, holistic information about the tree health status acquired and analyzed from Remote Sensing techniques can be collected.

Despite the fact that the traditional visual inspections are more accurate in detecting the defect inside the trees, Remote Sensing techniques are relatively efficient and cost-friendly which can be used to acquire the preliminary information of the tree and hence to sort out the most problematic trees and accompanied by the decision making of the Chartered Arborist for further inspection. In addition, Remote Sensing approaches allow quick tree risk assessment; therefore, the tree hazard can be minimized and thereby mitigate the damage and loss resulting from tree collapse.

## 1.2 Main Objectives

The purposes of conducting the project of introduction to the applications of Remote Sensing techniques on tree health monitoring are as follows:

- I. To briefly explain the basic principle of the Remote Sensing techniques applying in the tree health monitoring.
- II. To illustrate the overall methodology of monitoring the tree health condition by means of Remote Sensing techniques.
- III. To compare the three Remote Sensing techniques generally on the tree health detection.

### 1.3 Project Methodology and Framework

With a view to introducing the Remote Sensing approaches used for tree health monitoring, this project focuses on three major techniques, and therefore the project is constituted by three major parts, including (I) thermal infrared imaging, (II) hyperspectral imaging, and (III) multispectral aerial imaging. The overall project framework is shown in *Figure 1.1*.

In part I – thermal infrared imaging, for the data collection, infrared thermography of each selected tree will be captured using an infrared camera under field observation. Afterwards, it is necessary to convert the data format for further image processing including the tree trunk extraction. After this, the recognition of temperature change along the tree trunk will be focused. If there is a sharp variation of temperature, the area will be highly suspected as the tree's potential defective area, thereby determining the tree health condition.

In part II – hyperspectral imaging, similarly, the hyperspectral image of each chosen tree will be acquired using hyperspectral imaging camera through field observation. Then, it is followed by the identification of vegetation by way of the thresholding with NDVI. The tree crown can be extracted for further processing. The decision tree classifier will be adopted to classify the tree health status given the threshold value with quantitative variables. Typically, several vegetation indices other than NDVI will be applied to adequately use the vast portion of the electromagnetic spectrum sensed by the hyperspectral imaging camera.

In part III – multispectral aerial imaging, the digital aerial photo with near-infrared (NIR) band is the primary data source. Then, the vegetation area will be identified and extracted through a threshold value with NDVI. Hereafter, in healthy leaves determination, the NDVI threshold is applied based on the previous research. Therefore, it can separate the healthy and unhealthy leaves and determine the healthy and unhealthy tree crown and eventually the overall tree health condition of a particular tree.

The description of the methodology of each approach will be further illustrated in the corresponding chapters including *Chapter 3*, *Chapter 4*, and *Chapter 5*.

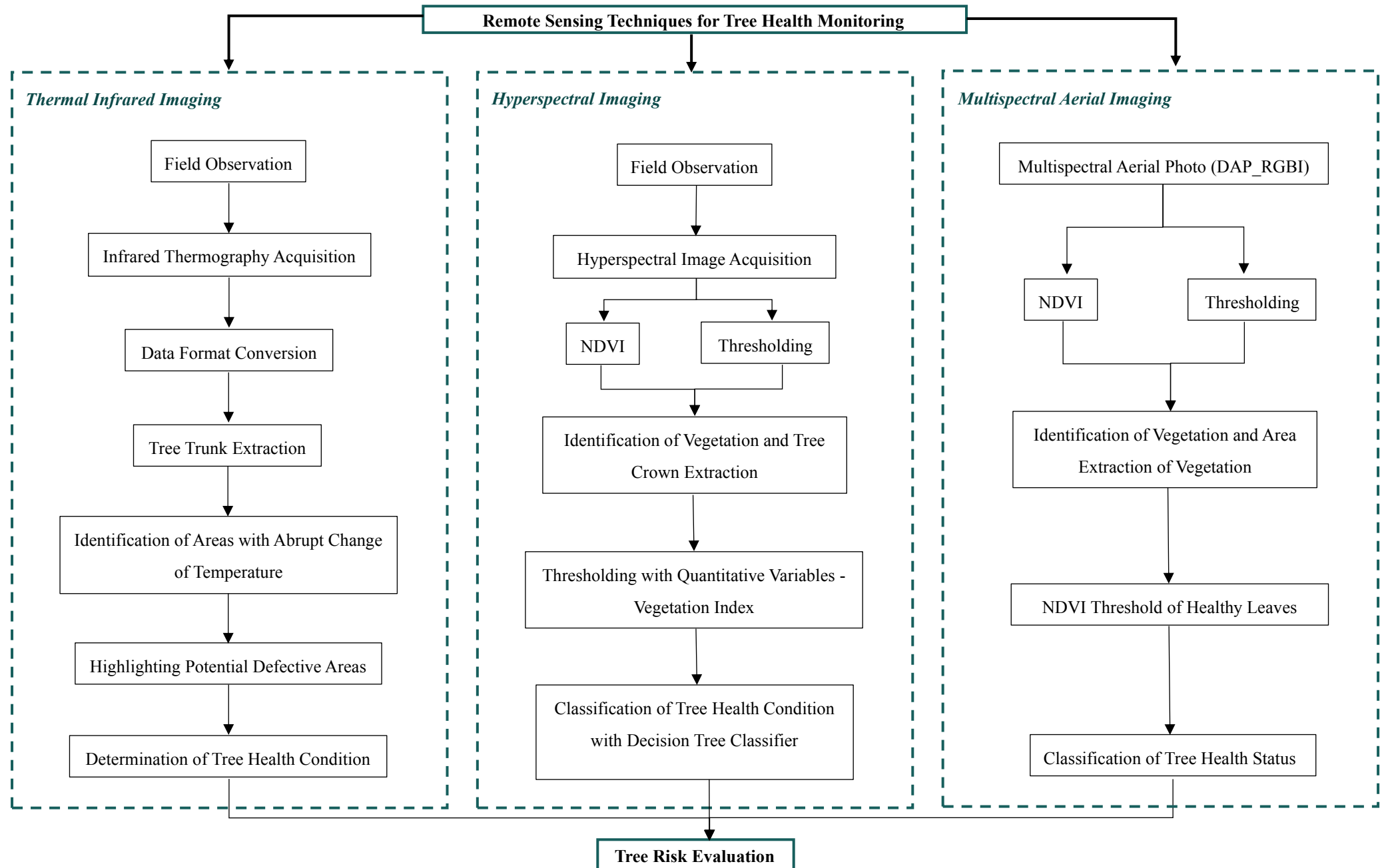


Figure 1.1. The framework of the methodology of this project

## 1.4 Structure of Project and Report

This report is structured into eight chapters. Chapter 1 introduces the background information, objectives, and overall project methodology. Chapter 2 gives the holistic reviews including basic concepts of the unhealthy tree, thermal infrared imaging, hyperspectral imaging, multispectral aerial imaging, etc. Chapter 3 presents the tree health monitoring through thermal infrared imaging with methodology and result presentation. Chapter 4 demonstrates tree health monitoring through hyperspectral imaging with the corresponding procedure and data analysis. Chapter 5 illustrates tree health monitoring through multispectral aerial imaging with methodology and result introduction. Chapter 6 points out the details regarding tree health detection by combining three Remote Sensing techniques. Chapter 7 provides the corresponding recommendation to the tree health monitoring in Hong Kong. Chapter 8 concludes the major findings from this study.

## CHAPTER 2 LITERATURE REVIEW

---

To commence with, the literature review of this study focuses on four major parts. First, the review of the basic concept of the unhealthy tree was discussed. Then, in the second part, more details of thermal infrared imaging were illustrated, while in the third part, hyperspectral imaging was described. In the last part, the basic concepts of multispectral aerial imaging were illustrated.

### 2.1 Basic Concepts of Unhealthy Tree

This project aims to figure out the health condition of the tree utilizing Remote Sensing techniques. In the following section, the fundamental concepts on detecting the tree healthiness will be discussed.

#### 2.1.1 Types of Tree Diseases

Trees are susceptible to diseases, where some diseases are considered mild to trees when it gets infected, yet it may only make the appearance not aesthetic. The disease can reduce productivity or kill the tree. When the defenses against disease are impaired, the disease may gain a foothold on the tree, causing infection and even death (University of Arkansas, 2020). The common reasons associated with disease problems are drought, overcrowding, and damaged stems or roots. Adequate water is necessary for the growth of the trees whereas root damage caused a reduction of water absorption ability. Root damage can provide an entrance for pathogens, and thus, the impediment of water absorption will increase the chance of tree infections for weakening tree healthiness.

Based on the University of Arkansas (2020) research, there are three categories of common tree diseases: foliage, stem, and root diseases in trees. For the foliage part, the fungal attack is the common disease that is fatal to trees, while other diseases may only cause an unpleasant outlook (McAlpine, 1899). Seasonal weather is one of the dominant factors that affect foliar, while Anthracnose is one of the common examples of foliar disease, it attacks the leaves and twigs on the trees, and sometimes the stem as well, especially in spring with lesions and blotches on leaves (Yoshida & Shirata, 1999).



**Figure 2.1.** Leaves deteriorated by Anthracnose (cited from the University of Arkansas, 2020)

For the stem part, the fungal attack is the common diseases on the stem, which is similar to the foliar diseases (McAlpine, 1899). Many of these diseases are fatal to the parts of the tree crown or the entire tree. Removal of the infected branches can save the tree in some circumstances. Canker is one of the examples of stem diseases. Many fungi cause cankers to live on the tree's surface, and the pathogens could enter the trees through natural or man-made wounds (Weingartner & Klos, 1975).



**Figure 2.2.** Diffuse cankers (Left) and Spot cankers (Right) (cited from the University of Arkansas, 2020)

For the root part, fungal disease is the main reason that causes lethal death to the tree (McAlpine, 1899). These diseases are usually fatal in the long-term as absorbing the water from the soil weakened by disease. Annosum root rot is one example of the fungus that can spread from the wound into the tree's root system by cutting the stump down, resulting in infectious from tree to tree (Oliva, Thor, & Stenlid, 2010).



**Figure 2.3.** Logging damage (cited from the USDA Forest Service, 2018)

### 2.1.2 Common Symptoms of Sick Tree

On the website of the Greening, Landscape & Tree Management Section of Development Bureau (2016), there are common tree health problems presented, which are divided into general conditions of the trees suffering from diseases and pests, improper cabling or another supporting system, leaning with buckling wood, composing fruiting bodies etc.

Apart from the general tree health problems, every tree has different structural defects that may lead to an unhealthy specimen (Boa, 2003). To be precise, the problems of each structure of the trees are diverse. For the crown, the indicators include dieback twigs on tree crown and topped tree. There are four indicators to be noticed for the branch: cracks of fissures on branches, cavities on branches, crossed branches and dead branches. For the trunk, swelling trunk (gall), co-dominant stems, included bark, multiple stems, the cavity and decay are mostly found in the trunk. For the root, invisible root collar, gridling root and restricted root growth are the indicators of tree problems (Perry, 1989).

Although there are some prominent and visible symptoms of tree defects, some trees' problems cannot be easily detected with naked eyes, such as internal decay. Different techniques are required to monitor tree health and categorized into low-risk and high-risk conditions (Meilleur, 2006).

## 2.2 Thermal Infrared Imaging

According to the studies conducted before, thermal infrared imaging has been applied in tree health detection for several years. Thus, the fundamental concept concerning infrared thermography will be discussed in the following aspects.

### 2.2.1 Thermography and Infrared Light

According to Norman (2004), infrared is the energy of heat that humans can only feel yet cannot be seen. All objects emit a certain level of infrared radiation. Thermal energy has a longer wavelength that human eyes cannot detect it. In order to make the thermal energy measurable and visible, thermal imaging cameras usually detect radiation in the long-infrared range of the electromagnetic spectrum (approximately 9 - 14  $\mu\text{m}$ ) and produce an image, called a thermogram, of that radiation. The amount of radiation emitted by an object is proportional to the temperature, and thus, the temperature variations are shown in thermal imaging. Therefore, thermal imaging is a method to make the energy emitted by any objects measurable and visible and this is termed as thermography.

### 2.2.2 Principal of Thermal Infrared Camera

Infrared thermography (IRT) is a non-contact, non-destructive, and non-invasive technique (Usamentiaga et al., 2014). It allows the detection of radiated heat energy from objects and bodies in the electromagnetic spectrum's infrared range. The conversion of infrared energy into visible imaging is processed through instruments that produce false-color images, such as an infrared camera that contains an optical system, focuses on infrared energy onto the sensor array. The infrared energy can be detected then converted into an electronic signal, after the camera processor's mathematical calculations. Each temperature value is assigned to a different colours, where a thermal image or video can then be generated; the temperature calculations can be performed by the image or video (Vidal & Pitarma, 2019).

When the camera views the object, it receives radiation from the object from the ambient between the camera and the object surface, and from the atmosphere itself, *Figure 2.4* illustrated the heat transfer processes involved in a thermographic measurement.

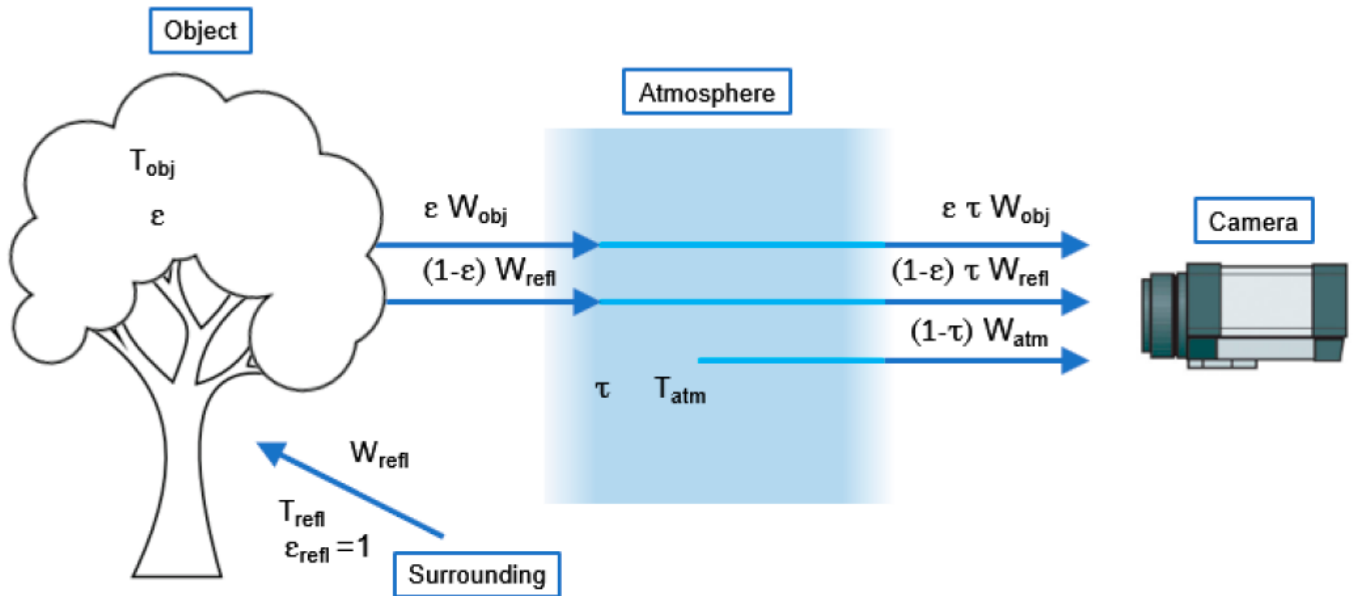


**Figure 2.4.** Schematic representation of a generic thermographic measurement (cited from Vidal & Pitarma, 2019)

An infrared camera can sense the heat precisely, allowing the user to monitor thermal activities and identify and evaluate relative heat-related problems.

### 2.2.3 Interpretation of Tree Health Condition under Temperature Differences

Thermography can record the tree's surface temperatures as thermal infrared images, pinpointing the cold spot on the infrared image of the tree trunk. The number of metabolic activities will affect the result of thermal infrared images. The uniqueness of living organisms is that they can extract energy from the environment and use it for activities such as movement, growth, and reproduction. The sum of the chemical reactions that occur within each cell of a living organism provides energy for vital processes and synthesizing new organic material (Kornberg, 2020). A healthy tree will have high metabolic activities that will show a higher temperature in the thermal infrared image, and vice versa. Therefore, thermal infrared images can correctly interpret tree health issues (Catena & Catena, 2008).

## 2.3 Hyperspectral Imaging

Hyperspectral imaging (HSI) is a widely applied technique in different industry fields, such as urban planning, precision agriculture, environmental management, etc. In the recent studies, HSI was utilized for tree health detection and monitoring (Degerickx et al., 2018).

### 2.3.1 Basis of Hyperspectral Remote Sensing

HSI collects and processes information across the electromagnetic spectrum (Chilton, 2014). It is also used to obtain each pixel's spectrum in the scene image and find objects, identify materials, or detect processes.

In HSI, the recorded spectrum has fair wavelength resolution and covers a wide range of wavelengths. According to Pu (2017), hyperspectral sensors measure continuous spectral bands. Multispectral imaging measures spaced spectral bands, which indicated that the hyperspectral sensor has better detection among different materials on land water and the atmosphere. The human eye can only see visible light colors in three bands (red, green, and blue), while spectral imaging divides the spectrum into more wavelength bands. This technique of dividing an image into bands can be extended beyond the visible range.

### 2.3.2 Sensor Resolution

Hyperspectral sensors collect information as a set of 'images'. Each image represents a narrow wavelength range of the electromagnetic spectrum, which is called a spectral band. In this section, the spatial, spectral and radiometric resolution will be discussed.

Spatial resolution is the smallest object's measurement value that the sensor can distinguish, or the ground area of the sensor with instantaneous field of view (IFOV) imaging, or the linear size of the ground represented by each pixel (Liang, Li & Wang, 2019).

The spectral resolution is the ability of a sensor to define finer wavelength intervals. Finer spectral resolution can result in a narrower wavelength range for a particular channel or band, resolving more spectral details (Gibson, 2000).

The radiometric resolution of an imaging system is its ability to discriminate very slight differences in energy. It will be more sensitive to detect a small difference in reflected or emitted energy if the radiometric resolution is finer (Gibson, 2000).

### 2.3.3 Vegetation Studies Under Hyperspectral Data

Hyperspectral Remote Sensing plays a crucial part in analyzing vegetation's reflectance in recent twenty years (Adam, Mutanga, & Rugege, 2010). Anderson (1970) researched on spectral discrimination of wetland species, while the spectral difference is inconspicuous in the visible band region between species, but more significant in the near-infrared region.

When solar radiation reaches the leaves, the reflection, absorption and transmission may occur. All vegetation species have the same essential components affecting its spectral reflectance, including chlorophyll and other light-absorbing pigments, water, proteins, starches, waxes, and structural biochemical molecules, such as lignin and cellulose (Kokaly et al. 2003). Reflectance and transmittance of vegetation are usually high in the near-infrared region and water absorption is high in the mid-infrared region. The high spectral resolution of vegetation shows some physical characteristics of vegetation. A vegetation spectrum can be subdivided into three regions. *Figure 2.2* shows the visible light region (400-700 nm) with high absorption, the near-infrared region (700-1300 nm) with low absorption, and the mid-infrared region with characteristic water absorption bands (1300-2600 nm). The characteristics can be used to discriminate plant species and with its statuses such as age, health, or phenological state (McCoy, 2005). Kumar (2001) indicated that different spectral bands of vegetation and visible light define chlorophyll and carotene absorption. The red edge region shows plant biochemical and biophysical parameters. The near-infrared (NIR) region reflects internal leaf structures. The mid-infrared region indicates water absorption and minor absorption of biochemical content. However, high spectral resolution data means highly redundant and poses significant challenges in developing methodologies suitable for vegetation discrimination (Hu et al., 2019).

## 2.4 Multispectral Aerial Imaging

Multispectral aerial imaging is the third Remote Sensing approach used for tree health monitoring in this study, while multispectral aerial image or multispectral satellite image is common for vegetation detection, management, and monitoring.

### 2.4.1 Basis of Multispectral Remote Sensing

Multispectral Remote Sensing involves acquiring visible, NIR, and SWIR images in several wavelength bands. Different materials reflect and absorb at different wavelengths. As such, it is possible to differentiate among materials by their spectral reflectance signatures as observed in these remotely sensed images.

### 2.4.2 Introduction to Vegetation Index

The Vegetation Index (VI) is the spectral transformation of two or more bands, aiming to enhance vegetation properties' contribution and realize reliable spatial and temporal inter-comparisons of terrestrial photosynthetic activities canopy structure changes (Huete et al., 2002). Many vegetation indices take advantage of the inverse relationship between red and near-infrared reflectance associated with healthy green vegetation.

The Normalized Difference Vegetation Index (NDVI) is a simple vegetation indicator, which can be used to analyze Remote Sensing observation (Pettorelli, 2013). It usually radiates from a space platform and to observe whether the target contains live green vegetation.

The range of NDVI is between -1 to 1. For the vegetation, the range of NDVI typically is 0.1 to 0.9; for the barren area of rock, sand or snow, the range would be 0 to 0.1; for the shrub and grassland, the range would be 0.1 to 0.3; for the temperate and tropical rainforests, the index value would be 0.3 to 1.0.

## CHAPTER 3 TREE HEALTH MONITORING THROUGH THERMAL INFRARED IMAGING

---

### 3.1 Introduction

Invasive or destructive techniques are usually used to diagnose the screening structure and intervene after visual inspection. Three methods were introduced in this project for tree health monitoring. In this chapter, thermal infrared imaging will be presented. The basic principle of thermal infrared imaging is a method or device that can detect the infrared energy emitted from the surface, converting it into temperature and display the temperature field image for further analysis (Usamentiaga et al., 2014). The basic concept behind is that all objects, no matter living and non-living, have a temperature above absolute zero (0 K) and emit infrared radiation, captured by a device capable of converting this energy into a picture. The internal structure of the body exhibits different thermal behaviors, depending on the health of its parts. Furthermore, infrared thermal imaging technology (IRT), which is going to introduce in this section, is a non-invasive technology. This technique had shown advantages when it applied in the inspection of trees to detect degradation or voids other techniques may damage their structure, stability and durability. Infrared thermal imaging (IRT) is a promising technique used to inspect trees. It highlights the differences to interfere with the thermal patterns of trees. In common with other non-destructive methods, IRT neither distinguishes the type of damage nor the cause of the damage. However, it can identify healthy and deteriorating tissues with thermograms, distinguish from healthy tissues, and observe the tree whether it is a functional body as a whole. IRT is a non-contact technology that allows the detection of damaged tissue in real-time. It is based on the detection of thermal differences between healthy and damaged zones.

In 1984, Dr. Giorgio Catena and his group started a pioneering survey on the use of thermal infrared scanners to monitor tree health based on the trunk's temperature. From the scan performed by Catena (1990), it can be confirmed that the presence of external cavities or dead tissues that constitute internal discontinuities will produce corresponding surface temperature changes. For example, the temperature of trees with larger external cavities is lower (dark spot). Compared with the neighboring bark, a cluster of small scars is recorded, which has a higher temperature (lighter shadow spots). Therefore, it can be concluded that this technique can effectively reveal the cavities and dead tissues in the trunk (Catena, Palla, & Catalano, 1990). In light of this, according to ongoing research by Catena (1990), a thermograph of the trunk of a seemingly healthy tree shows several areas of cooler temperature (darker grey spots), using a Pressler auger to drill it into the trunk to confirm whether there is a cavity and further ensure the effectiveness of the method.

Moreover, it not only shows the existence of the cavity, but also reveals the range and size of the pathogen's activity on the tissue. Catena (1993) proposed that this method can distinguish bark defects and rot. Bark defects displayed in thermograms can easily be mistakenly identified as internal decay during a surface inspection as they can display as low-temperature areas, and different types of bark, such as plain, wrinkled, cracked would be presented differently in the thermogram. However, by inspecting the superficial damage on the bark, such as decortication, scar tissue, and observing the appearance of the bark's thermal image before the image is taken, these actions can help identify the cause of temperature changes and avoid

misunderstandings (Catena, 1993). Since then, the theory that thermal imaging cameras can be used to determine and identify defects in the external cavity, internal cavity and bark has been established, and many studies conducted by Catena have also provided evidence for this theory.

Besides, according to Potter and Andresen (2002), the heat flow in the tree stem involves various processes. First, the conduction inside the tree is affected by density, temperature and thermal conductivity. The second is the convective heat transfer between the atmosphere and the surface of the trees. When the trees' surface temperature is different from the ambient temperature, heat gain and loss will occur when hot or cold air blows. Therefore, wind speed and the radius of trees are the factors that affect convective heat transfer. Third, heat flow within the tree trunk is influenced by the incident solar radiation at a point on the tree's surface controlled by solar zenith, azimuth angle, and incidence angle. All these vary within a day, the day of the year, and the tree trunk point. In addition, the emission and absorption of infrared radiation are also involved in the heat flow in the tree stem, which is affected by the incoming radiation from the surrounding features, and the ambient temperature is similar to the surrounding features.

All in all, the heat flow within the stem of a tree is affected by species, its moisture content, atmospheric absorption characteristics, temperature and wind speed. Moreover, Derby and Gates (1966) pointed out that the texture of the bark affects the convective heat transfer, thereby affecting the heat flow in the roots and the temperature of local areas on the trunk.

This chapter introduces the application of IRT for inspection of the health of trees. This chapter will mainly focus on analyzing tree health monitoring by applying thermal infrared imaging, and the result will be investigated. It was conducted using traditional methods and captured each tree manually with only one tree at a time. A description of the IRT application for inspection of trees and several experiments are explained.

### 3.2 Study Area

In this chapter, the research field of using thermal infrared imaging for tree health monitoring is in Causeway Bay. As above-mentioned, thermal infrared imaging will be conducted tree by tree, thus, in this project, the trees inside the Victoria Park and Cotton Path will be focused. For the Victoria Park, spinning Latitude  $22^{\circ}16'55''$  to  $22^{\circ}17'00''$  N and Longitude  $114^{\circ}11'09''$  to  $114^{\circ}11'29''$  E, *Figure 3.1* shows the location and boundary of the Victoria Park. In addition, there is a tree located in Cotton Road where *Figure 3.1* presents the location.

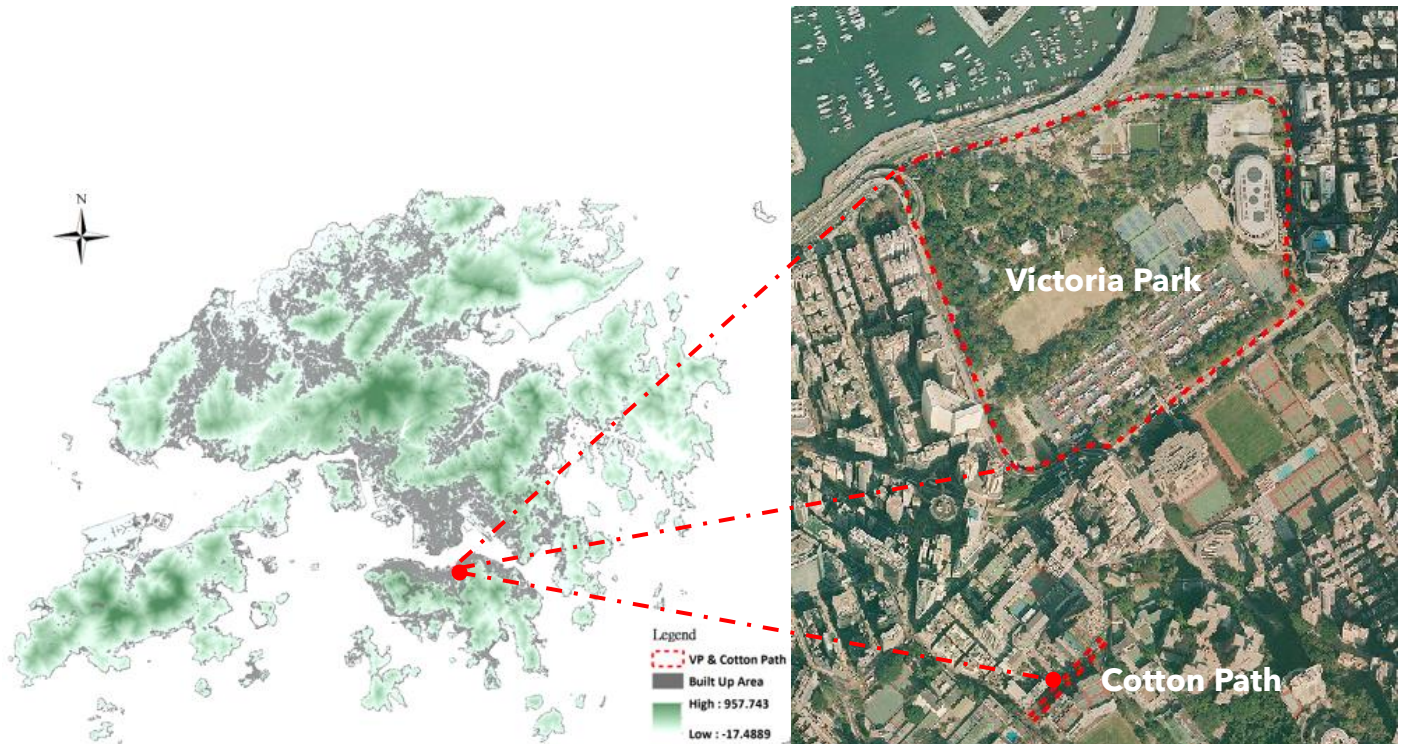


**Figure 3.1.** Location of Victoria Park and Cotton Path

### 3.3 Overview of Data and Equipment

All data used in this chapter were acquired through field operations. In this project, the portable thermal imaging camera, called FLIR T650sc, is utilized. For the thermal imaging camera's temperature range, the normal maximum temperature is  $150^{\circ}\text{C}$  and the normal minimum temperature is  $-40^{\circ}\text{C}$ . The details of the IRT are shown below.

IRT from TLIR T650sc	
Acquisition Data	2020/08/11
Equipment	FLIR T650sc
Resolution	640 x 480 (pixel)
Width	480 pixels
Height	640 pixel
Object Temperature Range	-40°C to 150°C or +100°C to 650°C
Average Data Size	1.41 MB
Accuracy	$\pm 1^{\circ}\text{C}$ or $\pm 1\%$ of reading for limited temperature range for measuring object within $+5^{\circ}\text{C}$ to $+120^{\circ}\text{C}$ and ambient temperatures of $+10^{\circ}\text{C}$ to $+35^{\circ}\text{C}$ ( $+49^{\circ}\text{F}$ to $+95^{\circ}\text{F}$ )

**Table 3.1.** Metadata of the IRT acquired by FLIR T650sc

The FLIR T650sc is shown in *Figure 3.2*.



**Figure 3.2.** FLIR T650sc (FLIR, 2020)

### 3.4 Methodology

Conceptually, to investigate the tree health condition of each selected tree, five major steps are required. In the preparation stage, target tree selection was conducted. Afterward, in the data acquisition, there is the field observation with data collection using FLIR T650sc. Then, it is followed by data pre-processing. Subsequently in the result analysis, the data interpretation can be executed to classify the tree health status of the trees. *Figure 3.3* shows the overall workflow of this section. More details about the methodology are discussed in the following section.

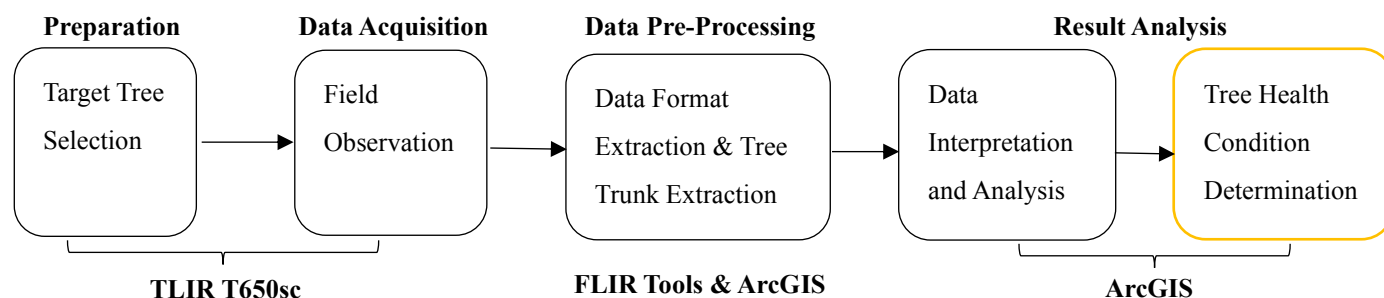


**Figure 3.3.** The overall workflow of this section

#### 3.4.1 Data Acquisition

Before the commencement of the data acquisition, site reconnaissance is necessary to have a conspectus of the site. With the site reconnaissance, the fieldwork details should be considered, such as which location can provide both samples of healthy and unhealthy trees.

The thermal infrared images were taken by the thermal imaging camera FLIR T650sc (as shown in *Figure 3.2*), which has a high level of accuracy of  $\pm 1$  °C (FLIR, 2020). And the date of conducting fieldwork was on August 11, 2020, and the weather condition of that day was cloudy, which is satisfied with the requirements for taking thermal infrared images.

##### 3.4.1.1 Target Tree Selection

In this project, the Old and Valuable Trees (OVTs) are prioritized, and those data can be searched from Tree Register, a website provided by the Greening, Landscape & Tree Management Section of the Development Bureau. Moreover, the Hong Kong government has set up a registry of OVT, the qualification for OVT is based on the age, size, species, and sometimes, the shape of the individual tree (Development Bureau, 2016). For the tree with healthy conditions, the data can be obtained from the website of “Tree Register”, and the targeted healthy trees demonstrated in this project are located in Victoria Park and the details of the trees are shown in *Table 3.2* and *Figure 3.4*. Health condition of trees in the urban area of Hong Kong is monitored regularly, which may be difficult to find enough trees having health problems. In order to be able to search for more samples of unhealthy trees, observation during fieldwork is required. In the project, two unhealthy trees

were selected, located in Victoria Park with the government’s information, and one of the samples located in Cotton Path, the details information is shown in *Table 3.2* and *Figure 3.4*.

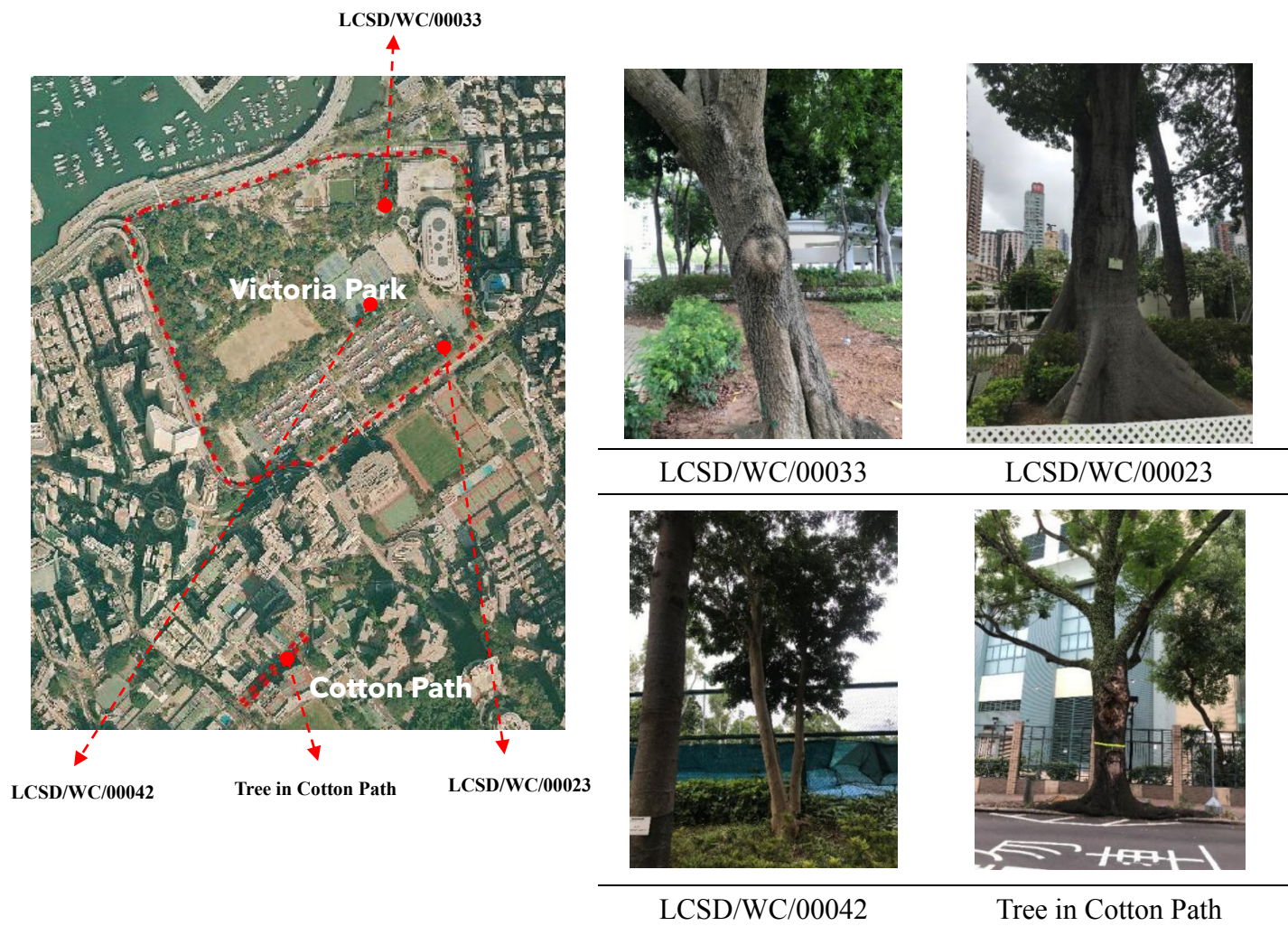


Figure 3.4. Location of the selected trees

Details of the Tree	LCS/D/WC/00023	LCS/D/WC/00033	LCS/D/WC/00042	Tree in Cotton Path
Location	Victoria Park	Victoria Park	Victoria Park	Cotton Path
District	Wan Chai	Wan Chai	Wan Chai	Wan Chai
Tree Species	Ceiba Pentandra	Mimusops Elengi	Fraxinus Americana	/
Tree Status	Alive	Alive	Alive	Alive
Condition	Health condition (good)	Health condition (good)	<ul style="list-style-type: none"> <li>- Dieback twigs (&lt; 5%)</li> <li>- Cavity (severe)</li> <li>- Health condition (fair)</li> <li>- Dead branches</li> <li>- Obvious wound(s)</li> </ul>	<ul style="list-style-type: none"> <li>- Large wound(s)</li> <li>- Decay</li> </ul>

Table 3.2. Properties of the selected tree

### 3.4.1.2 Field Observation

The tree inspection was carried out by applying qualitative IRT at the passive mode, that is, the heat source was the ambient environment through solar radiation (Catena, 1990). Heat flows from the hotter area of the tree to the colder area. By observing the thermal pattern's irregularities on the tree surface, the existence of defects, voids, and deteriorated tissue can be noticed (Bellett-Travers & Morris, 2010).

Data collection is to capture the images of different tree trunks using a thermal camera, while different health conditions of the tree can be reflected in the thermal image. In this project, four tree trunks were captured, two are healthy and two in unhealthy conditions.

### 3.4.2 Data Pre-processing

#### 3.4.2.1 Tree Trunk Extraction

The process of tree trunk extraction was processed in ArcMap. In this project, manual-based segmentation is applied to extract the tree trunks by removing the background information, and the detailed pre-processing steps are presented below to get the segmented tree trunks.

1. Add the TIFF file into ArcMap;
2. Create a shapefile (.shp) and delimit the area of tree trunk;
3. Use the function of Raster Clip to extract the area of interest (AOI);
4. Save the clipped tree trunk as a TIFF file.

The extracted tree trunk can be processed for the analysis afterwards. *Figure 3.5* shows the extracted result of the tree trunk and the temperature difference shown in the image is more significant and obvious.

Also, in accordance with the following figures, the temperature difference is not significant due to the influence of the irrelevant contained background. Therefore, tree trunk extraction is essential. After the extraction, the temperature difference of the tree trunk is more obvious, and it would be better for the tree health analysis.

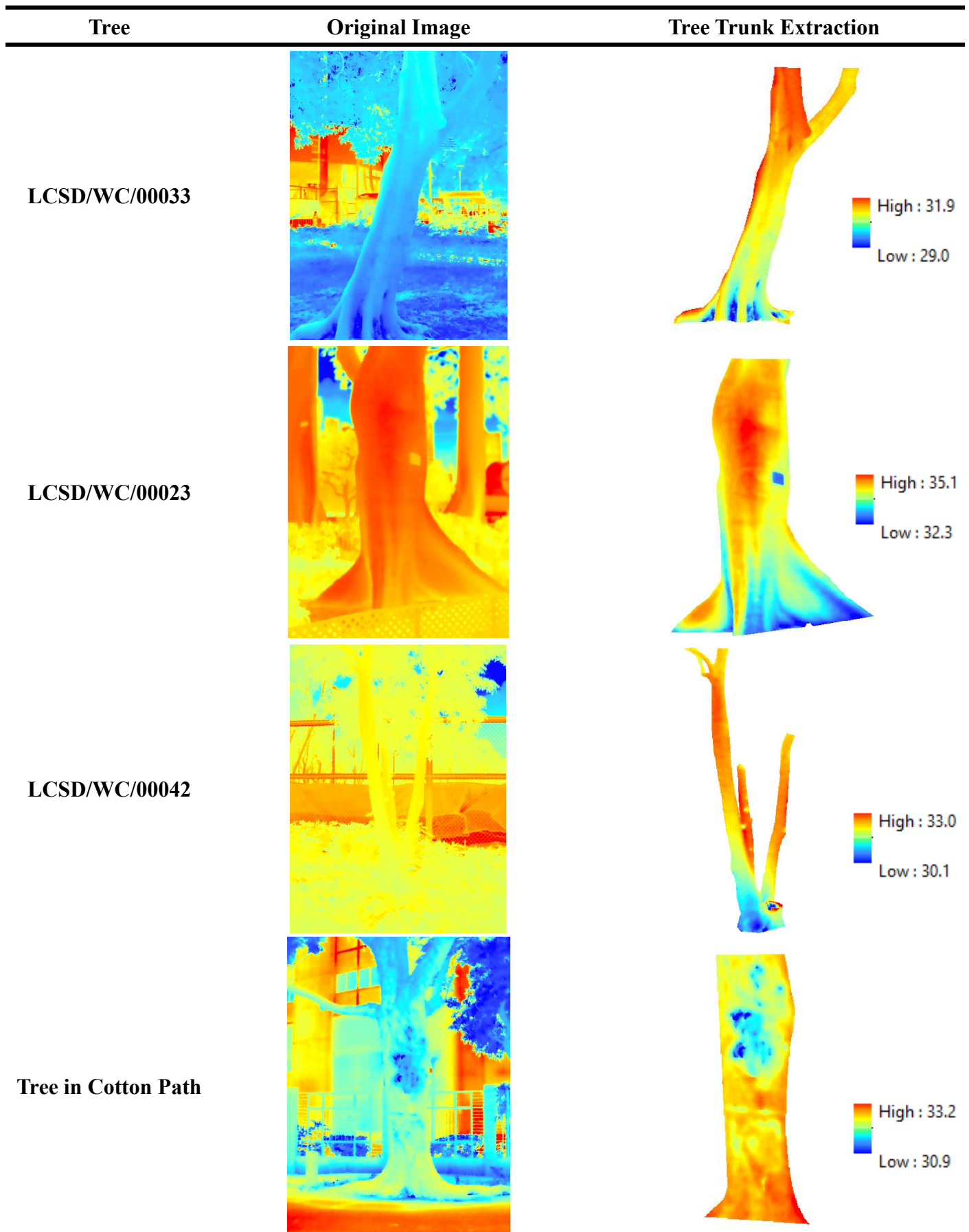


Figure 3.5. Result of tree trunk extraction

### 3.4.3 Data Interpretation and Analysis

From the below figures presented in *Section 3.5*, it can be seen that a healthy tree has a higher temperature, and the unhealthy tree, the temperature of the tree trunk is lower than the healthier one, the below figures indicated that a healthy tree trunk maintains high metabolic activities that resulted in higher temperatures. For the unhealthy tree trunk, which was injured, it resulted in a lower temperature due to the lack of metabolic activity.

Based on the aforementioned concepts, trees maintain a balanced relationship with the ambient temperature, thus, when the solar heating effect exceeds the temperature of the trees is usually lower than the atmospheric temperature (Bellett-Travers & Morris, 2010). Therefore, from the above figure, the trees showing in *Figure 3.5* show higher temperatures in the healthier parts, and lower temperatures in the degraded parts and parts that have been recently wetted by water (Meola, 2012). By spotting and analyzing the temperature difference shown on the thermal image, the interpretation of the target trees' health condition can be noticed. Only the temperature on the tree bark's surface can be represented when the thermal camera captured the thermal contrast. Nevertheless, the tree bark near deteriorated tissue and voids show a lower temperature than the area around it (Catena & Catena, 2008). IRT can detect the significant differences in the wood and tree bark's thermal properties and it is often applied to trees and offers a means to differentiate damaged and deteriorated tissue from healthy tissues (Vidal & Pitarma, 2019).

## 3.5 Result and Analysis

Following those mentioned above, this section will discuss the characteristics of the healthy and unhealthy tree presented in IRT. In view of this, tree health monitoring using thermal infrared imaging in the future can recognize the tree health status of a particular tree based on the characteristics.

### 3.5.1 Characteristics of Healthy Tree in Thermal Infrared Image

*Figure 3.6* presents the IRT of the *Mimusops Elengi* (LCSD/WC/00033) and *Ceiba Pentandra* (LCSD/WC/00023), which are the samples of the healthy tree. For the LCSD/WC/00033, the upper part of the tree has a higher temperature compared with the middle and lower parts of the tree. Also, there is a gradual change of temperature along the tree. The temperature decreased from the upper part to the lower part of the tree. In addition, there is no abrupt change but a smooth variation of temperature. Similarly, for the LCSD/WC/00023, the upper portion of the tree typically has a higher temperature, and it is gradually decreased from the upper area to the lower area near the root because of the sunlight heat. There is no sudden variation of temperature along the whole tree except the information tag located in the middle of the tree trunk.

*Figure 3.6* shows temperature changes in the area of the two sample trees under direct sunlight exposure (left upper zone of the tree) and areas in the shadow. For the LCSD/WC/00033, on the left of the trunk is TP1 under direct sun exposure at 31.5°C and TP2 at 31.1°C. The TP3, in the middle of the trunk, with 30.9°C. TP4 is at

the bottom of the trunk at 30.7°C where TP5 is located near the root at 30.3°C under the shade (*Table 3.3*).

The LCSD/WC/00023 also shows the temperature changes of areas under direct sun exposure and shadow areas. TP1, TP2 and TP3, are exposed to direct sunlight, the temperature is at 34.5°C, 35.1°C and 34.7°C respectively. For the part near the root with less sun exposure, TP4 and TP5, the temperatures of the point are at 33.9°C and 33.5°C respectively (*Table 3.3*).

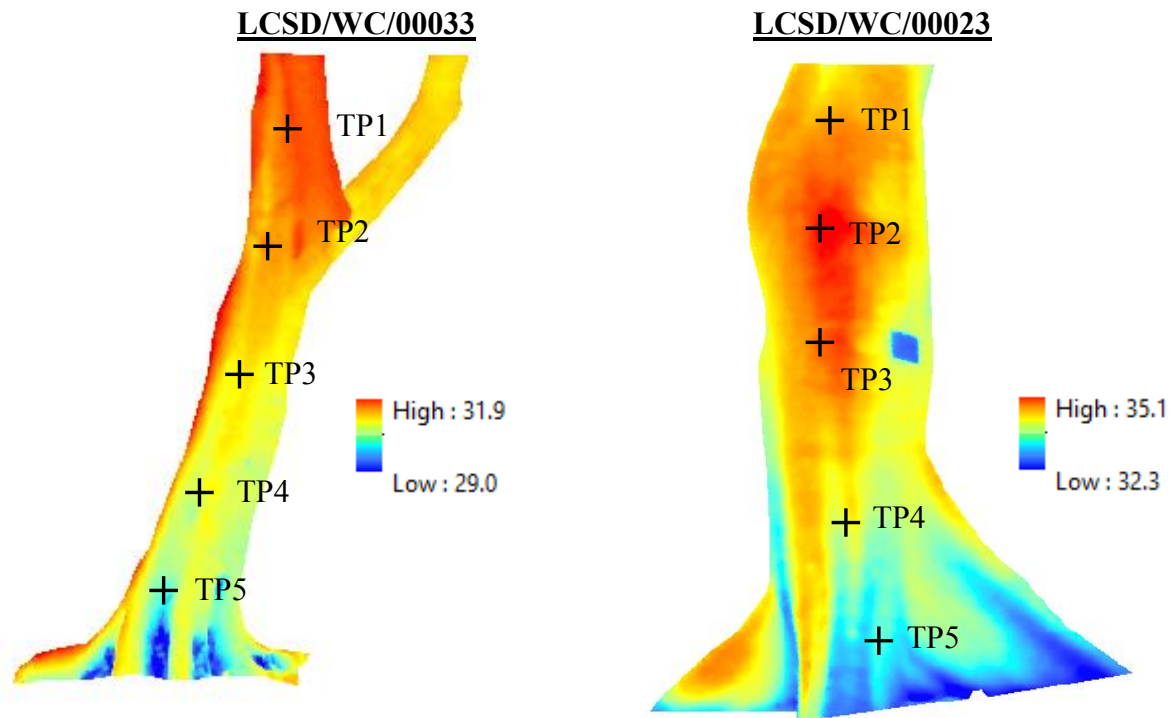


**Figure 3.6.** IRT of LCSD/WC/00033 (Left) and LCSD/WC/00023 (Right)

To indicate the characteristics of temperature variation in details, the quantitative presentation will be discussed and presented in *Table 3.3*.

IRT	Tree	Temperature (°C)				
		TP1	TP2	TP3	TP4	TP5
Figure 3.6 (Left)	LCSD/WC/00033	31.5	31.1	30.9	30.7	30.3
Figure 3.6 (Right)	LCSD/WC/00023	34.5	35.1	34.7	33.9	33.5

**Table 3.3.** Quantitative presentation of characteristic of the selected healthy tree

The above result indicated that when the tree is in a healthy condition, the temperature will increase or decrease gradually, and there will not be any temperature change abruptly, such as some parts will have a lower temperature than the surrounding area. Suppose some parts of the tree trunk show a sudden lower temperature than the other part of the tree trunk. In that case, it can be considered the tree trunk may have a condition such as a cavity, cracked etc. as mentioned in *Section 3.4.3*, with which the tree probably had an unhealthy condition and it will be discussed in *Section 3.5.2*.

### 3.5.2 Characteristics of Unhealthy Tree in Thermal Infrared Image

*Figure 3.7* presents the IRT of the selected unhealthy trees sample. For LCSD/WC/00042, the upper part of the tree (TP1), has a higher temperature compared with the middle (TP2) and lower (TP3) parts of the tree. From TP1 to TP3, a gradual change of temperature along the tree trunk is the same pattern of a temperature change as the healthy condition showing in *Section 3.5.1*. However, there is an abrupt change in the lower right part, which is the TP4 and TP5 located. From the below *Figure 3.7* (Left), TP4 has a higher temperature compared to TP5, which is different from the characteristics of the healthy tree. For the tree in Cotton Path, the temperature change is totally different due to the wound on the trunk. The IRT of the tree in Cotton Path indicated that the temperature of TP2, is the lowest compare to the other TPs where the wound was found. The IRT result indicated that some parts will have a sudden variation of temperature with a lower temperature than the surrounding areas when considered a defect by observing the abrupt change of temperature. In this case, those parts reveal a clue of possible deterioration or damage within the area.

Although both trees (LSCE/WC/00042 and Tree in Cotton Path) were under direct sunlight exposure, which was the same as the health trees samples, the temperature variation pattern is totally different from the healthy trees. For the LCSD/WC/00042, all TPs were under direct sun exposure, where TP1 was at 32.5°C, TP2 at 32.2°C, TP3, near the bottom of the trunk, with 31.8°C. TP4 is also near the bottom of the trunk at 33.0°C, TP5 is located in the hole of the trunk, at 30.7°C (*Table 3.4*). For the tree in Cotton Path, all TPs were under direct sun exposure. For TP1, TP3, TP4 and TP5, which are exposed to direct sunlight with no wounds and cracks, the temperatures are at 32.7°C, 32.9°C, 32.7°C and 33.0°C respectively. For the damaged part, which is TP2, the temperature of the point is at 31.2°C that the temperature is relatively lower than the surrounding areas (*Table 3.4*).

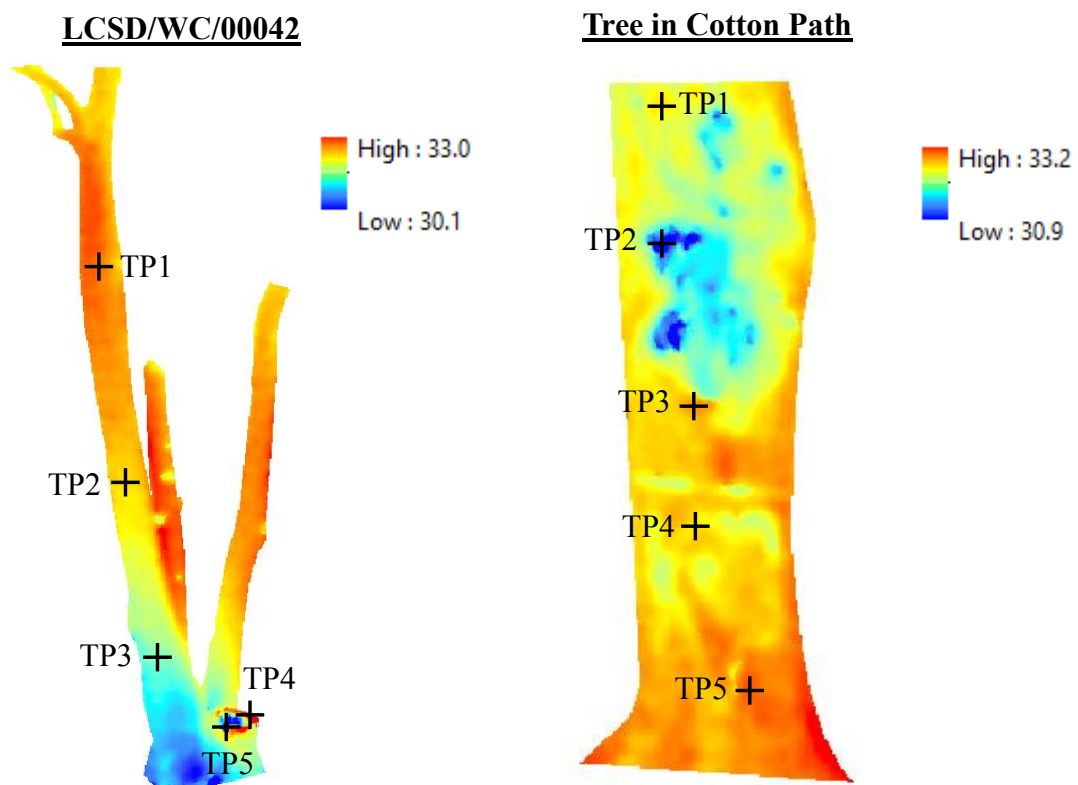


Figure 3.7. IRT of LCSD/WC/00042 (Left) and Tree in Cotton Path (Right)

With a view to indicating the characteristics of temperature variation in details, the quantitative presentation of the selected unhealthy tree will be discussed and presented in *Table 3.4*.

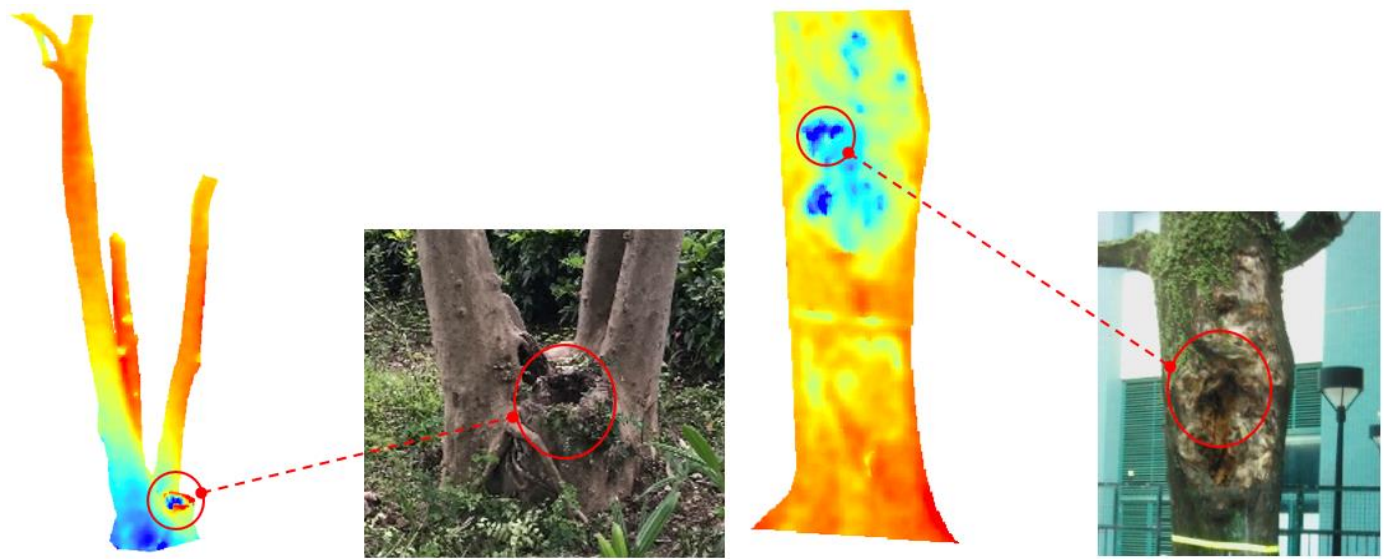
IRT	Tree	Temperature (°C)				
		TP1	TP2	TP3	TP4	TP5
Figure 3.7 (Left)	LCSD/WC/00042	32.5	32.2	31.8	33.0	30.7
Figure 3.7 (Right)	Tree in Cotton Path	32.7	31.2	32.9	32.7	33.0

Table 3.4. Quantitative presentation of characteristic of the selected unhealthy tree

The above result indicated that contrary to healthy trees, the temperature of the unhealthy part of the tree usually will have an abrupt change compared to the surrounding areas, which means the unhealthy part will have a lower temperature than the healthy part of the tree trunk. An abrupt temperature change strongly indicates the tree has possible deterioration while a healthy tree would not occur abruptly in IRT temperature. To ensure the IRT and the temperature changes on those TPs indicating the trees' deterioration or not, the photos of the sample trees should also be evaluated simultaneously with the IRT.

Figure 3.8 shows the photos of the LCSD/WC/00042 (Left) and tree in Cotton Path (Right), this strong evidence was confirmed with observations of an enormous interior cavity linked to the hole and wound, where both TP5 of LCSD/WC/00042 and TP2 of tree in Cotton Path have a lower temperature than the surrounding areas, which are relatively healthy compared to these two points. By considering both IRT and the photos of the sample trees, the result revealed subtle differences in the temperature in the thermograms, resulting from

the bark pattern, pruning wounds, etc. Those parts appeared as spots of slightly lower temperatures than the adjacent areas. The photos must also be required to conduct IRT techniques as it is a visual inspection tool that helped facilitate thermograms' interpretation.



**Figure 3.8.** IRT of LCSD/WC/00042 (Left) and Tree in Cotton Path (Right)

Based on the above samples, there are several conditions, including exposure to sunlight and shadow; thermal contrast between the environment and the object targeted; the moisture like rainfall; vegetation covers such as mosses and lichens; typical bark patterns of each species; the thermal comparison between the trunks of different caliber within the same tree, are required to consider having an accurate result of tree health detection using thermal infrared imaging (Pitarma, Crisóstomo, & Ferreira, 2019). Suppose there is an apparent sudden variation of temperature, and the conditions mentioned above do not cause the change. In that case, it is highly expected that there is a defect within the tree.

### 3.6 Chapter Summary

IRT is considered a tool to check the health of trees. Although the types of damage cannot be determined, it has proven to be a useful tool for detecting damage early. In addition, thermal imaging cameras can diagnose trees without causing any damage to the tree. As other non-invasive and non-destructive techniques, pathogens can also be identified using invasive methods. However, the comparison of inspection methods shows that IRT has great advantages in distinguishing between functional and dysfunctional organizations, thereby inspecting the vitality and health of trees. Moreover, compared with other methods, the thermal infrared camera method can reduce labor costs and the cost of conducting detailed investigations. It can evaluate most trees, allow simultaneous surveys, and monitor pathological changes quickly, economically, and non-destructive. With the development of IRT and increased applications, improved results can be achieved. Its correct application requires in-depth multidisciplinary knowledge of phenomena and technology understanding in common with any other technology.

## CHAPTER 4 TREE HEALTH MONITORING THROUGH HYPERSPECTRAL IMAGING

---

### 4.1 Introduction

Traditionally, the visual tree assessment (VTA) method is applied to examine tree health conditions (Mattheck & Breloer, 1994). Applying Remote Sensing technology is an alternative for tree health monitoring. Remote Sensing technology can provide quantitative and spatially continuous information that covers the entire city at once and can be easily replicated over time.

According to Mobasheri, Rezaei, & Valadan Zoej (2007), the hyperspectral sensor acquires information about objects. Since there are a large number of narrow continuous bands, it can accurately survey the vegetation biochemical and environmental parameters for effective research. The spectral reflectance of natural surfaces is sensitive to the special chemical bonds of material molecules in different solid, liquid, and gas states. Since hyperspectral data is spectrally determined, it provides enough spectral information to identify and distinguish spectrally unique materials. They can be used to measure important plant quality parameters in farmland and plantation. Since most natural features have special spectral signals, these special signals appear in a very narrow area of the electromagnetic spectrum, so hyperspectral sensors can capture those subtle changes and have greater advantages than broadband sensors. In a hyperspectral image, each pixel has its own spectrum, generating a map of the presence and abundance of chemical junctions on the pixel (Dutta et al., 2009).

This chapter introduces the application of hyperspectral imaging for inspection of the tree health. For that purpose, this section is structured as follows. This chapter will mainly focus on analyzing the monitoring tree healthy by applying hyperspectral imaging, including the study area, procedures, and the result will be analyzed. The hyperspectral imaging application for inspection of trees and several experiments are discussed.

### 4.2 Study Area

In this chapter, the research field of the introduction of hyperspectral imaging for tree health monitoring covers part of the Causeway Bay. As mentioned above, hyperspectral imaging will be conducted tree by tree; thus, in this project, the tree inside Victoria Park will be focused. However, as the trees inside Victoria Park are well-managed and most are under a healthy condition, the selection of the surrounding trees should also be included to demonstrate the example of the discussion of an unhealthy tree. For the Victoria Park, they were spinning Latitude 22°16'55" to 22°17'00" N and Longitude 114°11'09" to 114°11'29" E, with a 100m buffer zone for the surrounding trees. *Figure 4.1* shows the location and boundary and the 100m buffer zone of Victoria Park.



Figure 4.1. Boundary of the study area

### 4.3 Overview of Data and Equipment

In this project, the portable hyperspectral imaging camera, named Specim IQ, is utilized. The details of the Specim Dataset are shown below.



Figure 4.2. Specim IQ (SPECIM, SPECTRAL IMAGING LTD, 2020)

Specim Dataset from Specim IQ	
Acquisition Data	2020/09/13
Equipment	Specim IQ
Resolution	512 x 512 (pixel)
Width	512 pixels
Height	512 pixels
Wavelength band	400 - 1000 nm
Data Format	Specim Dataset with ENVI compatible data files
Field of View (FOV)	31 x 31 deg

**Table 4.1.** Metadata of the Specim Dataset acquired by Specim IQ

In addition, the equipment used in this method is a portable hyperspectral imaging camera, with the model Specim IQ, which allows users to define how the camera is used and how the hyperspectral data is processed, analyzed, saved, and visualized. Specim IQ is shown in *Figure 4.2*.

#### 4.4 Methodology

The methodology is discussed in *Section 4.4.2.1* and *Section 4.4.3*. *Figure 4.3* indicates the overall workflow of this study.

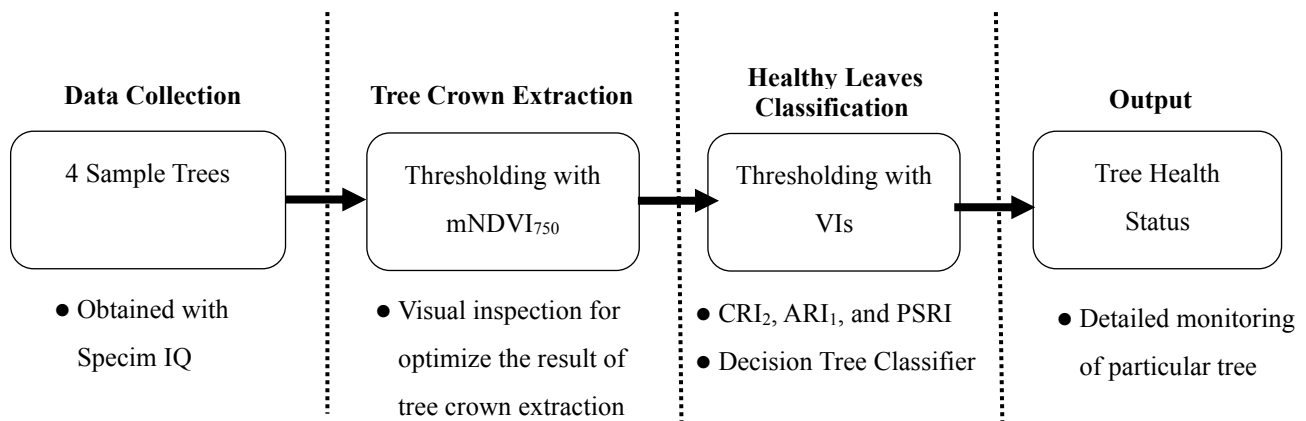


**Figure 4.3.** Overall workflow of this study

##### 4.4.1 Data Acquisition

The data acquisition process can be started by taking hyperspectral images by the hyperspectral camera Specim IQ (*Figure 4.2*). And the date of conducting fieldwork was on September 13, 2020, and the weather condition of that day was sunny, which is satisfied with the requirements for taking hyperspectral images.

### 4.4.1.1 Target Tree Selection

In this project, 2 healthy trees, and 2 unhealthy trees were selected, located inside Victoria Park and the surrounding roadside near Victoria Park. As aforementioned, the trees inside Victoria Park are usually under healthy conditions; therefore, the surrounding trees near Victoria Park should also be considered. The detailed tree information is shown in *Figure 4.4*.

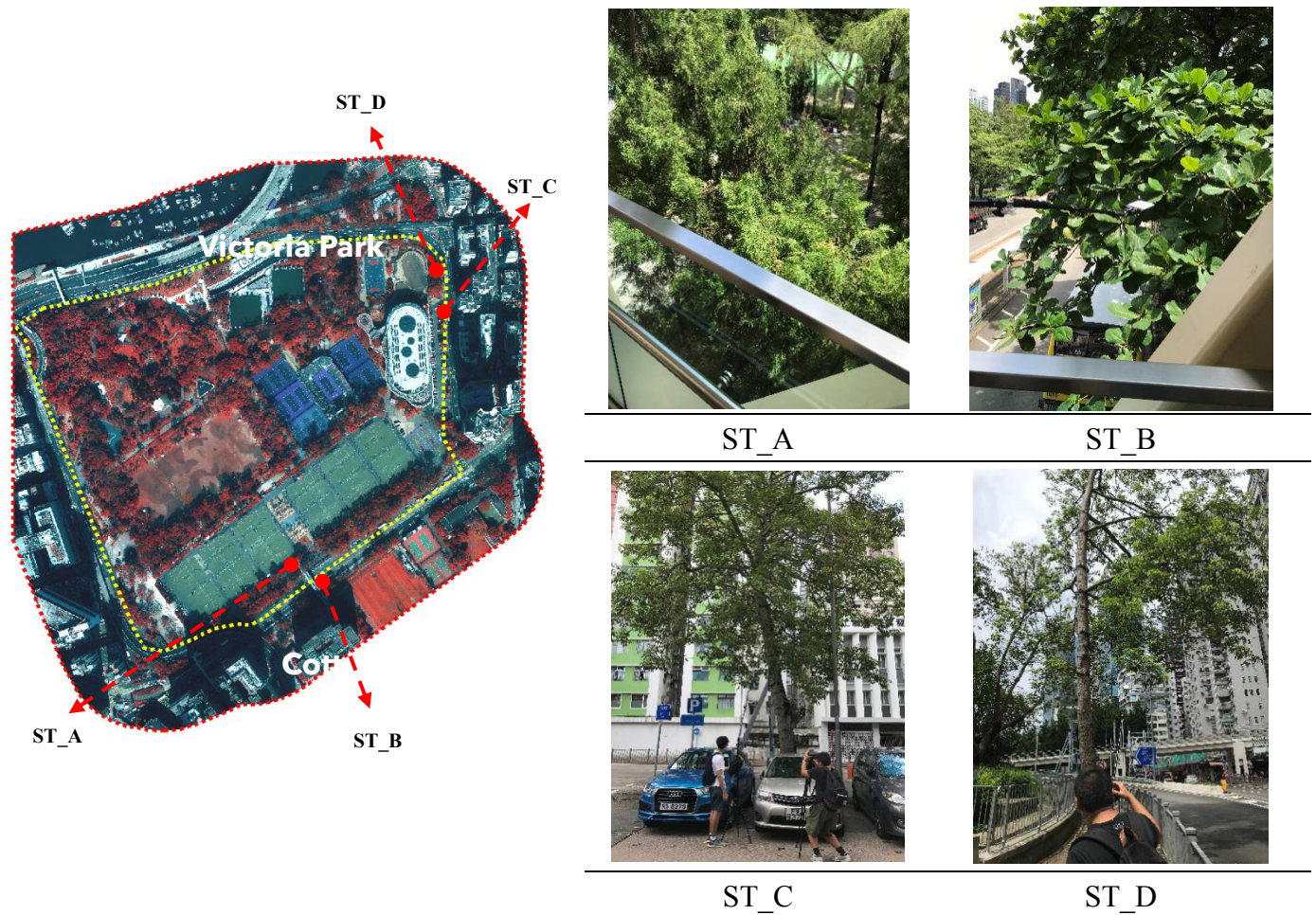


Figure 4.4. Location of the selected trees

#### 4.4.1.2 Field Observation

Hyperspectral imaging is rapidly entering the mainstream of Remote Sensing and applied Remote Sensing research. The hyperspectral system is possible to collect hundreds of spectral bands in one acquisition, resulting in more detailed spectral data (Govender, Chetty & Bulcock, 2007).

Data collection is to capture the images of different tree canopies using a hyperspectral camera. Different health conditions of the tree can be reflected in the hyperspectral image by determining the tree canopy condition and analyzing the different indices afterwards. In this project, four tree canopies were captured, two are in a healthy condition, and two are unhealthy.

During the field observation, the white reference must be included in the hyperspectral images as shown in *Figure 4.5*. By using the hyperspectral camera for obtaining the spectral reflectance characteristics, the sensor calibration is required based on reference reflectance panels, such as the aforementioned white reference. White reference and the features, such as tree crown, were acquired under the same spectral and spatial condition to generate the final calibrated hyperspectral images. The white reference placement should also be parallel to the target feature to simulate the same absorption and reflectance of the electromagnetic radiation.



ST\_A



ST\_B



ST\_C



ST\_D

Figure 4.5. RGB of the four sample trees

## 4.4.2 Data Pre-processing

Before detecting the tree health status of the selected tree, it is necessary to extract tree crown area, especially the tree crown. Accordingly, a more precise tree health detection can be done without the influence of the non-vegetation pixel. In light of this, in the following sections, *Section 4.4.2.1*, the vegetation index and the threshold utilized for this purpose will be discussed.

### 4.4.2.1 Identification of Area of Vegetation

The vegetation index with narrow bands will be adopted to extract the tree crown and use the hyperspectral image. Due to the spectral reflectance of the vegetation is different from other features, especially the Red and NIR; therefore, Modified Red Edge Normalized Difference Vegetation Index (mNDVI<sub>750</sub>) can be used to

identify the tree crown area.

According to Gitelson and Merzlyack (1994),  $NDVI_{750}$  is termed as the difference between the reflectance at 750 nm (related to the scattering of the internal structure of the leaf) and the reflectance at 705 nm (associated with the absorption of leaf chlorophyll), normalized by dividing the sum of these reflectances. In addition, the revised red-edge normalized vegetation index ( $mNDVI_{705}$ ) compensates for high leaf surface scattering by subtracting the reflectance at 445 nm from all  $NDVI_{750}$  formulas (chlorophyll and carotenoid absorption produce the minimal reflectance) (Sims & Gamon, 2002). The index is sensitive to small changes in leaf cover, areas without vegetation and plant senescence.

The equation of  $mNDVI_{705}$  is as follows:

$$mNDVI_{705} = \frac{(750nm - 705nm)}{(750nm + 705nm - (2 * 445nm))} \text{-----(a)}$$

Based on Dutta et al. (2009), the common range for vegetation is normally between values of 0.26 to 1.0, thus, in this study, this range will be adopted to extract the tree crown for further tree health classification. *Figure 4.6* presents the result of tree crown extraction.

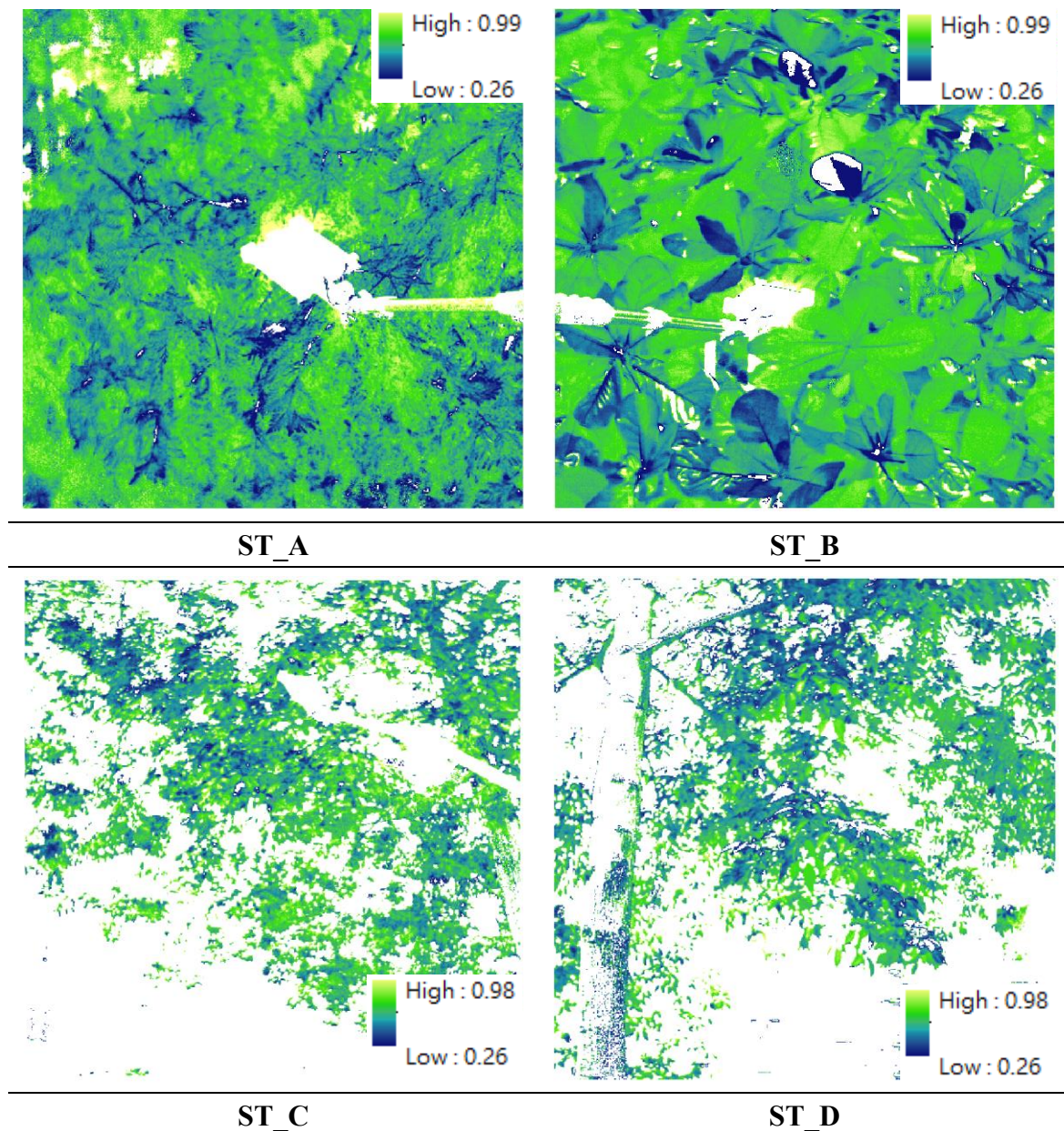


Figure 4.6. Result of tree crown extraction

#### 4.4.3 Healthy Tree Crown Detection

Pigments, water, and other biochemical substances absorb specific radiation wavelengths, thereby reducing these areas' reflectivity. The spectral absorption properties of pigments are reflected in the leaves' reflection spectrum, which provides the opportunity to use the measurement of reflected radiation as a non-destructive method for quantifying pigments. However, due to overlapping absorption characteristics of pigments and other components, it may be challenging to correlate the reflectance at a single wavelength with an available pigment concentration. In addition, due to differences in internal structure, surface and moisture content, leaf reflectivity can vary independently of pigment concentration. Hyperspectral indices can detect features that affect vegetation health based on the absorption bands in the vegetation spectrum of each pixel and individual pixels. *Table 4.2* listed the indicators used in this study. These indicators are Carotenoid Reflectance Index 2 (CRI<sub>2</sub>), Anthocyanin Reflectance Index 1 (ARI<sub>1</sub>), and Plant Senescence Reflectance Index (PSRI).

#### 4.4.3.1 Index for Thresholding of Healthy Leaves

For classifying a tree crown's health condition, three VIs were utilized and their basic concept with the equation will be discussed in the following. To commence with, for the Carotenoid Reflectance Index 2 ( $CRI_2$ ), carotenoids play a role in the light absorption process of plants and protect plants from the harmful effects of excessive light. Weakened vegetation contains higher concentrations of carotenoids, so this index is a measure of stress vegetation. The Carotenoid Reflectance Index is defined as the difference between the inverse reflectance at 510 nm related to the absorption of chlorophyll and carotenoids and 550 nm associated with the absorption of chlorophyll and anthocyanins (Gitelson, Zur, Chivkunova & Merzlyak, 2002).  $CRI_{700}$  uses the inverse reflectance at 700 nm, which is related to chlorophyll absorption instead of the inverse reflectance at 550 nm (Gitelson et al., 2002).  $CRI_1$  is an indicator of sensitivity to carotenoid pigments available in leaves and stems. Compared with chlorophyll, a higher  $CRI_1$  value means a higher carotenoid concentration.  $CRI_2$  is a modification of  $CRI_1$  that can provide better results in areas of high carotenoid concentration. A higher  $CRI_2$  value indicates a higher carotenoid concentration and the leaf is unhealthy. The equation of  $CRI_2$  is as the following:

$$CRI_2 = \left( \frac{1}{510nm} \right) - \left( \frac{1}{700nm} \right) \text{————(b)}$$

For the Anthocyanin Reflectance Index 1 ( $ARI_1$ ), anthocyanin is a water-soluble pigment that is abundant in new leaves and senescent leaves. The concentration of anthocyanins in weakened vegetation is higher, so this index is for measuring stress vegetation. The anthocyanin reflectance index (ARI) is defined as the difference between the inverse reflectances at 550 nm and 700 nm (Gitelson, Merzlyak & Chivkunova, 2001).  $ARI_1$  is an index sensitive to reflectivity based on the anthocyanin content present in the leaves. The increase in  $ARI_1$  indicates that the leaves change through new growth or death (Gitelson et al., 2001). This index uses reflectance measurements in the visible spectrum to take advantage of the absorption characteristics of stress-related pigments. The equation of  $ARI_1$  is as the following:

$$ARI_1 = \left( \frac{1}{550nm} \right) - \left( \frac{1}{700nm} \right) \text{————(c)}$$

Based on  $CRI_2$  and  $ARI_1$ , when the rate of photosynthesis decreases due to plant stress, leaves show higher concentrations of carotenoids and anthocyanin pigments than chlorophyll pigments, and the higher leaf surface content of chlorophyll pigments is a response to low light use efficiency. It has been proved that the vegetation index based on the strips sensitive to these leaf pigments is closely related to the vegetative growth stage (i.e. leaf expansion or senescence) and the stress degree of the vegetation (Gamon, Penielas & Field, 1992). Due to the loss of chlorophyll pigment caused by nitrogen deficiency, stress may also interfere with the nutritional status of plants and ultimately change photosynthesis. Therefore, vegetation indices based on bands sensitive to the foliar concentration of nitrogen can also be used to track pressure-induced changes in plants (Fillela & Penuelas 1994). Chlorosis and necrosis are visual symptoms of a decrease in the amount of pigments in plant

leaves in response to some stress inducer. In stressed plants, green pigments (i.e. chlorophylls) have a greater decline compared with light yellow-orange-red pigments (i.e. carotenoids) and red-blue-violet pigments (i.e. anthocyanins). It causes unhealthy leaves (for example, green leaf disease) to change color. Further reduction of all pigments will brown the leaves, which indicates that the leaves of the plant are dead (i.e. necrosis). Suppose a consistent relationship is found between the vegetation index of the vegetation affected by specific stress factors and chlorosis and necrosis symptoms. In that case, the index can be used to detect, evaluate, and monitor the substance's damage to the same species in other areas (Penna and Altmann, 2009).

For the Plant Senescence Reflectance Index (PSRI), PSRI aims to maximize the indicator's sensitivity to large amounts of carotenoids for chlorophyll. An increase in PSRI indicates increased canopy stress (carotenoid pigments), the onset of canopy senescence, and plant fruit's ripening. Applications include plant health monitoring, plant physiological stress detection and crop production and yield analysis. The equation of PSRI is as the following:

$$PSRI = \frac{(680nm - 500nm)}{750nm} \text{ —————(d)}$$

By using the three VIs mentioned above, the suitable thresholds for classifying the tree health condition in accordance with the study of Dutta et al. and the summary of their equations are indicated and presented as the following table.

Vegetation Index	Index Equation	Threshold Range
CRI <sub>2</sub>	CRI <sub>2</sub> = (1/510nm) - (1/700nm)	1 - 11
ARI <sub>1</sub>	ARI <sub>1</sub> = (1/550nm) - (1/700nm)	0.001 - 0.1
PSRI	PSRI = (680nm - 500nm) / 750nm	-0.1 - 0.2

**Table 4.2.** Summary of VIs' equation and their threshold

Since each of the above indexes indicates specific plant parameters' characteristics, these indexes must be analyzed simultaneously to obtain accurate information. For this reason, the decision tree classification method is adopted in the second part of the study. It involves the recursive division of the feature space, based on a set of rules learned through the training set analysis. A tree structure was developed in which specific decision rules are implemented on each branch, involving one or more combinations of attribute inputs. Then, the new input vector classifies from the root node through successive branches until it is placed in a specific class. This method consists of several stages, among which we assign a class to each pixel through binary decision making in each stage through some mathematical conditions, thereby dividing the image into two classes. Each of these new classes will go through another stage and will be divided into two new classes, and so on. Each index and its defined thresholds and restrictions introduced by different sources can be applied through these stages. *Figure 4.7* shows the decision tree in this study.

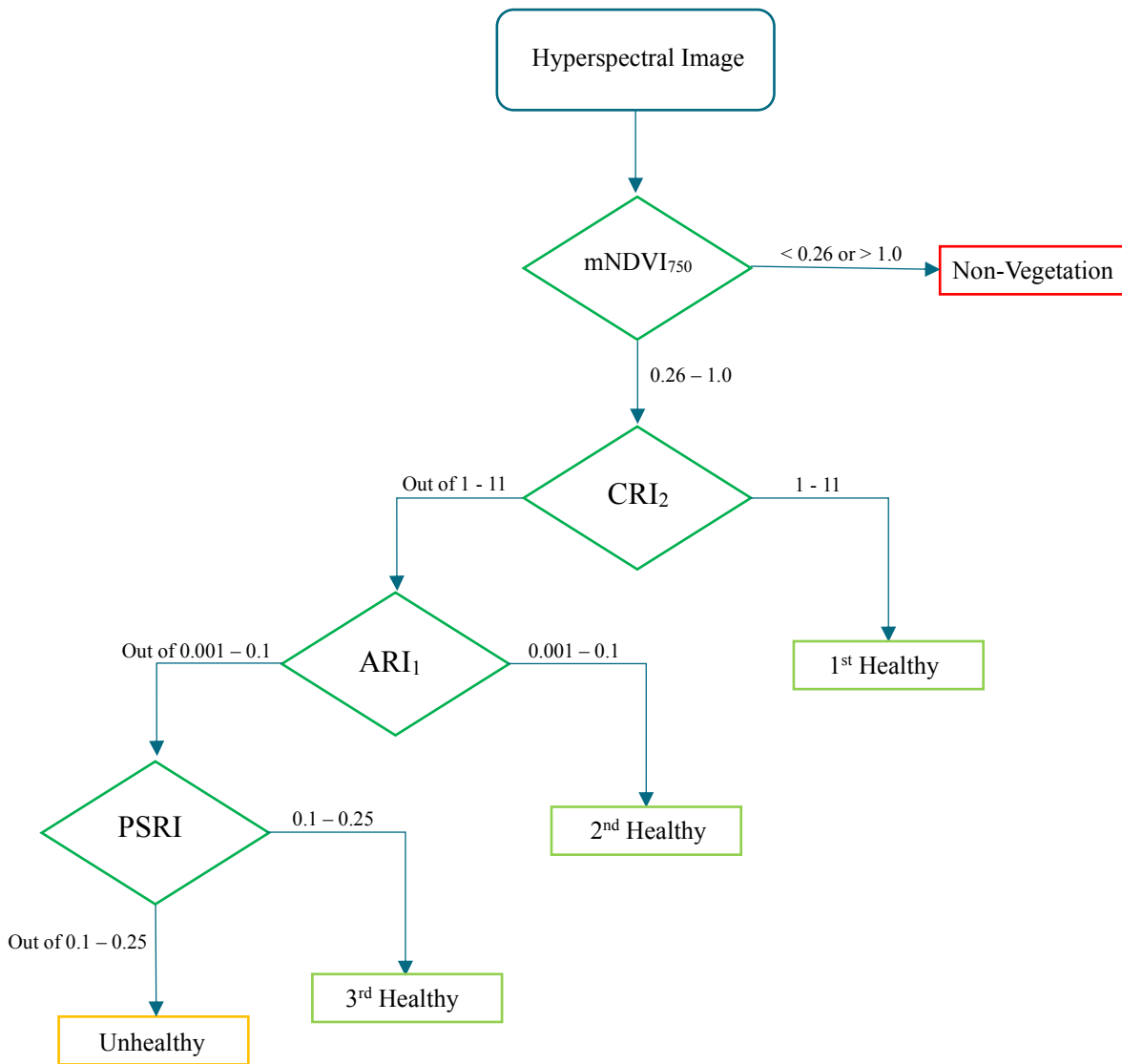


**Figure 4.7.** Decision tree of tree health condition classification

In this study, the threshold values of  $NDVI_{705}$  were applied first to separate the vegetated areas from non-vegetated regions. This image containing vegetation area was used as a mask for the rest of indices image. In the 2<sup>nd</sup> stage by using carotenoid ( $CRI_2$ ) for pigments other than chlorophyll. In the 3<sup>rd</sup> stage,  $ARI_1$  for anthocyanin content and in the 4<sup>th</sup>  $PSR_1$  for senescence have been applied to separate stressed and vegetation age into different classes. *Figure 4.7* shows the result of the image can be divided into 5 different classes, including non-vegetation, 3 classes of healthy and unhealthy.

## 4.5 Result and Analysis

According to the result of the decision tree, 5 different classes of each hyperspectral images were identified. The output image showed a high ability to monitor and study the growing and health of vegetated areas. In the classification result of the 4 sample trees, ST\_A and ST\_B have a similar result, and ST\_C and ST\_D have similar results. For ST\_A and ST\_B, it is clear that most of the pixel is classified as healthy and just a tiny portion is unhealthy. However, in contrast, ST\_C and ST\_D have a larger ratio of unhealthy pixels. *Figure 4.8* shows the classification result of the tree health condition of the 4 sample trees.

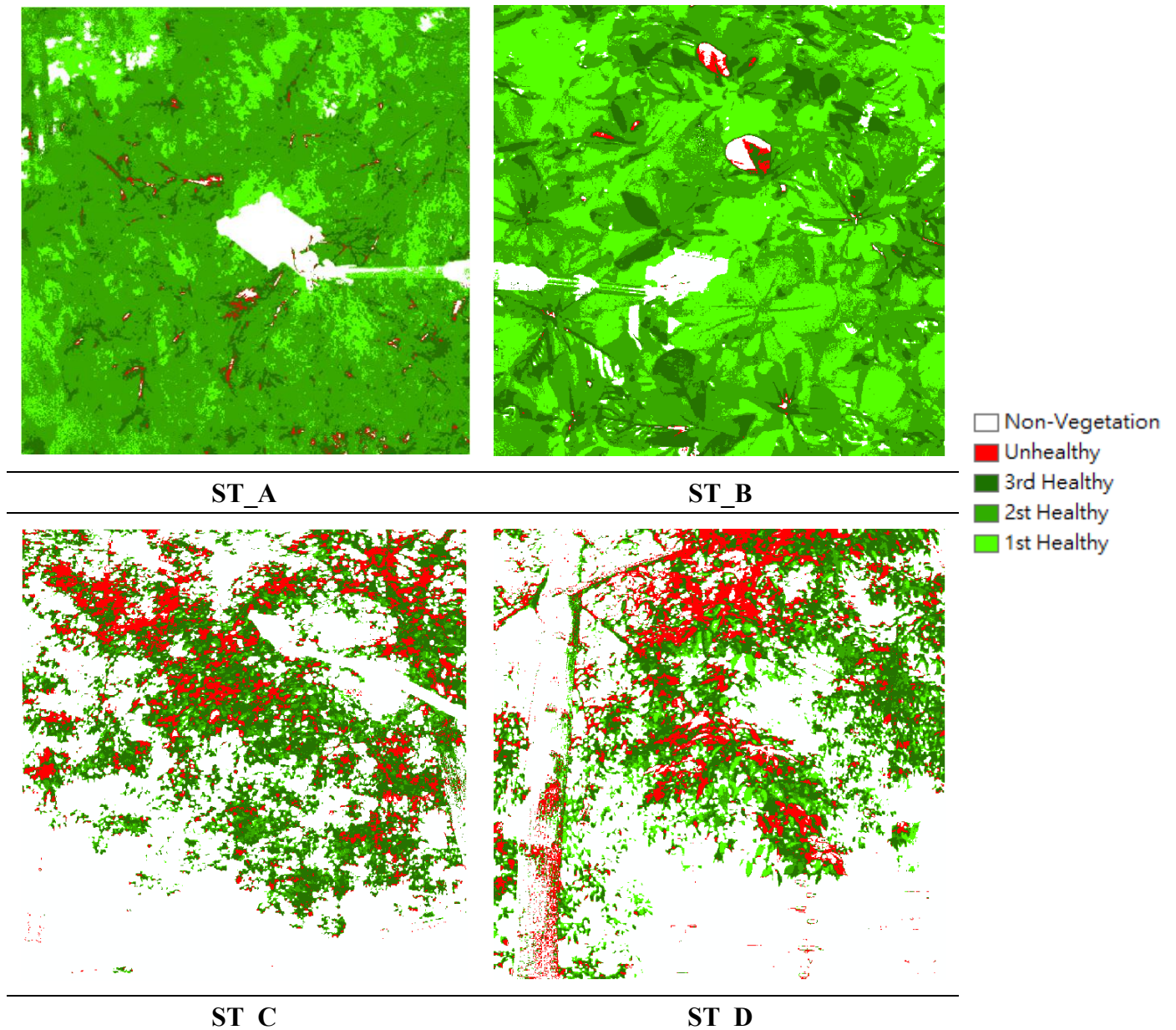


**Figure 4.8.** Result of tree health condition classification

Apart from the qualitative analysis, the quantitative presentation will be discussed below for a comprehensive understanding of tree health detection through hyperspectral imaging. It can be found that ST\_C and ST\_D

have around 20% unhealthy pixels, much more than that of the ST\_A and ST\_B. Table 4.3 presents the details of the classification result.

Tree	Pixel Level						
	Pixels				Percentage (%)		
	1 <sup>st</sup> Healthy	2 <sup>nd</sup> Health	3 <sup>rd</sup> Healthy	Unhealthy	Total	Healthy	Unhealthy
ST_A	42452	187098	22079	1795	253424	99.3	0.7
ST_B	96994	127150	27760	1210	253114	99.5	0.5
ST_C	7333	22999	58013	24729	113074	78.1	21.9
ST_D	17886	20191	44965	27157	110199	75.5	24.6

**Table 4.3.** Quantitative presentation of the tree health condition of the four sample trees

## 4.6 Chapter Summary

In this Section, a handheld hyperspectral camera was used to capture the tree crowns' hyperspectral reflectance. With the narrow spectral band, several VIs can be adopted to investigate a tree's health condition. For instance, the pigment concentration, senescence and carotenoids etc. are the critical parameters regarding the tree health. The threshold values for the abovementioned conditions were imposed and passed through a decision tree classifier to consider all the aforementioned hyperspectral indices together.

## CHAPTER 5 TREE HEALTH MONITORING BY MULTISPECTRAL AERIAL IMAGING

---

### 5.1 Introduction

Urban forest is an essential natural resource that affects most people living in the city. Trees in urban forests bring many benefits. It can provide aesthetic and recreational benefits and reduce air pollution and storm runoff, save energy, store carbon, provide UV protection, create habitats for wildlife, and maintain moderate temperatures (Xiao & McPherson, 2005). According to Xiao and McPherson (2002), the benefits stated above are affected by the healthiness of the trees, and tree health affects the function and performance of urban ecosystems directly. Traditionally, monitoring urban forest health relies on ground surveys and monitoring programs (Cumming et al., 2001).

Remote Sensing has been widely used in forestry studies (Erikson, 2004). Multispectral Remote Sensing data has spatial and spectral information of the land surface, which greatly promotes forest mapping, land cover and land use classification. According to Xiao, Ustin and McPherson (2004), the urban forest tree species mapping, high resolution spectral Remote Sensing data and multiple techniques can be applied in the city. With the aid of vegetation indices, such as the Normalized Vegetation Index (NDVI), Remote Sensing data has been extended to forest health mapping. It also has the potential to promote vegetation health research in urban areas (Maselli, 2004). High-resolution colour infrared Remote Sensing data have been widely used and these data are usually obtained from the three spectral windows: the near-infrared (NIR), red and green wavelength.

The tree health mapping deals with the spectral data of vegetation, representing the health of trees and other vegetation in the area of interest. A tree health map could be generated based on multispectral digital aerial photos, which combines classification, thresholding, and masking techniques to reflect trees' health status in the target area (Primicerio et al., 2015). The applied mapping technology is based on the difference in spectral response between healthy vegetation and unhealthy vegetation. Compared to the unhealthy vegetation, the healthy vegetation will reflect less in the red band of visible light but reflect more light in the NIR band (Xiao & McPherson, 2005). The main function of the tree health mapping is to identify the unhealthy urban trees, thereby determining the most concerned sick trees' manual inspection sequence.

In lieu of the traditional ground survey and on-site inspection method, tree health mapping offered an alternative to monitoring tree health in urban areas. This chapter introduces the application of multispectral aerial imaging for inspection of the health of trees. For that purpose, this section was structured as follows. This chapter will mainly focus on analyzing the monitoring tree healthy by applying multispectral imaging, including the study area, procedures, and results. Also, this is an area-based method; therefore, a large number of trees can be monitored at a shorter time comparing with thermal infrared imaging and hyperspectral imaging with handheld equipment. A description of the multispectral aerial imaging applied for inspection of trees and several experiments will be discussed.

## 5.2 Study Area

In this chapter, the research field for introducing tree health monitoring using multispectral aerial imaging is similar to the study area in *Chapter 3* and *Chapter 4*. Due to the target area is Victoria Park, the digital aerial photo covering Victoria Park is obtained, and the area is shown as *Figure 5.1*. The geographic coordinates in WGS84 of the study area are from Latitude  $22^{\circ}16'37''$  to  $22^{\circ}17'14''$  N and Longitude  $114^{\circ}11'06''$  to  $114^{\circ}11'36''$  E. And in HK80, the area is extended from 815311.133mN to 816527.372mN and 837184.440mE to 837989.833mE.

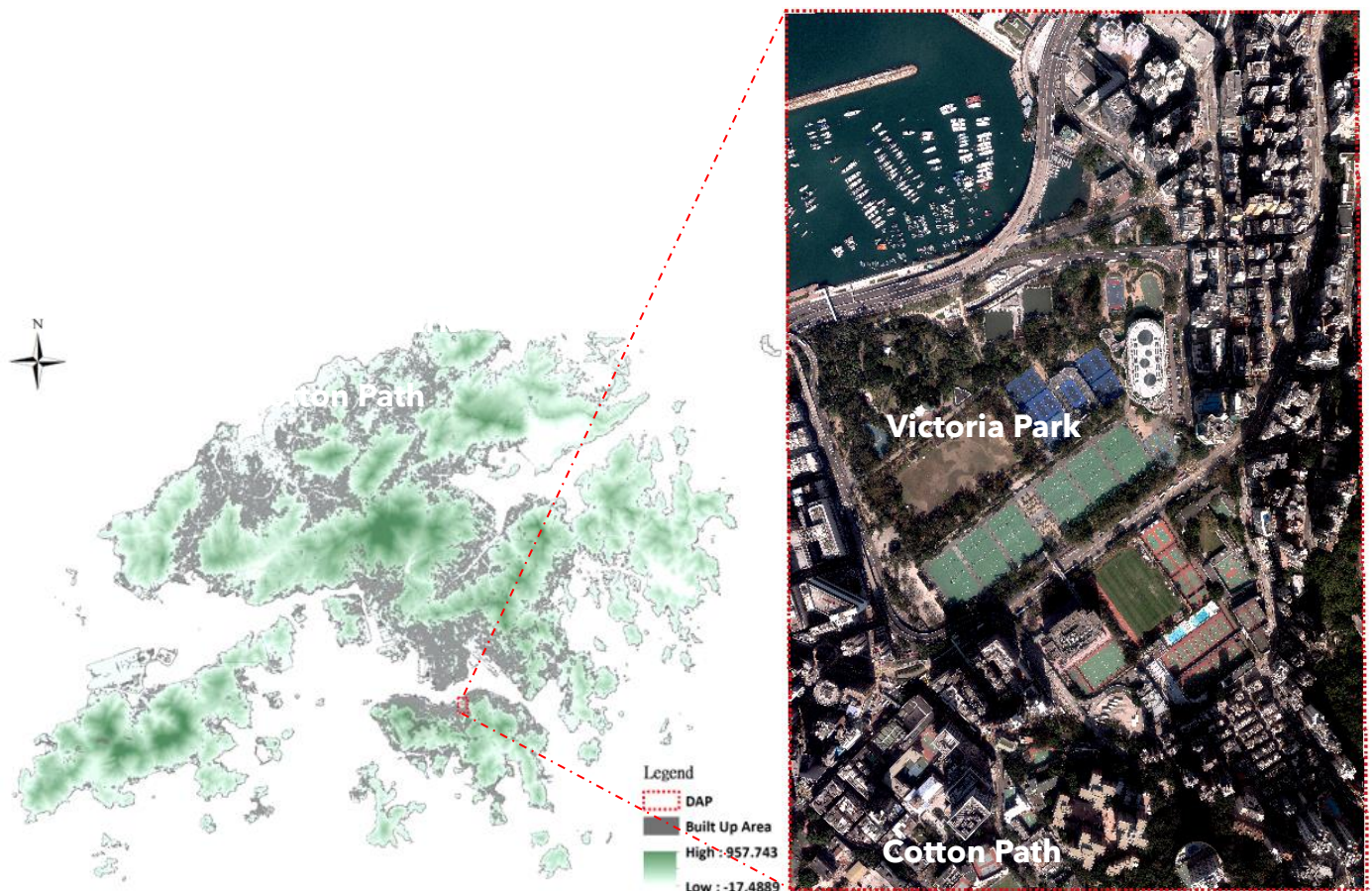


Figure 5.1. Spatial extent of the DAP

## 5.3 Overview of Data

Digital Aerial Photo (DAP) was acquired from the Survey and Mapping Office (SMO) of the Lands Department to conduct the analysis. Digital aerial photographs are one of the SMO digital map products. According to SMO (2018), the Digital aerial photos (UE version) is a digital aerial photo taken by a large-format digital aerial camera that was put into use in mid-2016 by the Lands Department. Digital aerial cameras can simultaneously collect five spectral band information (panchromatic, red, green, blue, and near-infrared) with a dynamic range of more than 12 bits. In this project, DAP\_RGBI will be used for performing tree health monitoring by using multispectral aerial imaging. DAP\_RGBI is a digital aerial photograph stored in a 16-bit file format, composed of four spectral bands (red, green, blue, and near-infrared). The data file size of each digital aerial photo is approximately 2 GB. It is the original photo without any color correction or color balance.

This original photo retains the original colors of digital aerial photos, which is conducive to the spectrum's analysis and research. *Table 5.1* presents the properties regarding the data of this section.

<b>DAP_RGBI - E056347</b>	
<b>Flight Date</b>	2019/01/25
<b>Equipment</b>	UltraCam Eagle
<b>Resolution</b>	20010 x 13080 (pixel)
<b>Spatial Resolution</b>	0.040m x 0.094m
<b>Spectral Resolution</b>	4 Bands (Red, Green, Blue, NIR)
<b>Radiometric Resolution</b>	16 Bit
<b>Spatial Extent</b>	Top: 816532.651mN, Bottom: 815306.830mN; Left: 837184.455071mE, Right: 837989.764mE
<b>Data Format</b>	TIFF
<b>Average Data Size</b>	1.97 GB
<b>Price</b>	\$355

**Table 5.1.** Metadata of the DAP

## 5.4 Methodology

This chapter presents two major parts for conducting the tree health monitoring and mapping using multispectral aerial imaging, identifying areas of vegetation and tree healthy detection. Both parts will be mentioned in *Section 5.4.1* and *Section 5.4.2*. *Figure 5.2* indicates the overall workflow of this study.

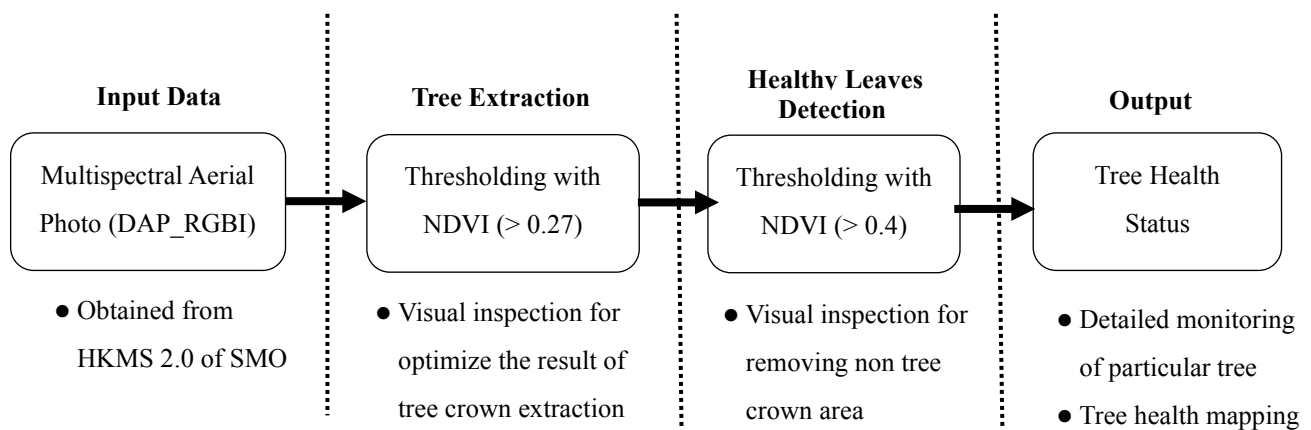


**Figure 5.2.** Overall workflow of this study

### 5.4.1 Identification of Area of Vegetation

Before detecting the tree health status of the tree located in the study area, it is necessary to extract the area of vegetation, especially the tree crown. Accordingly, a more precise tree health detection can be done without the influence of the non-vegetation pixel. *Section 5.4.1.1* and *Section 5.4.1.2*, the vegetation index, and the threshold utilized in this purpose will be discussed in the following sections.

### 5.4.1.1 Index for Vegetation Extraction

Remote Sensing data, such as multispectral aerial image is the principal data source for analyzing vegetation cover on a different scale. Together with the Remote Sensing techniques, such as ratio band and vegetation index, vegetation coverage in the study area can be figured out. According to the spectral reflectance curve, vegetation reflects the most in NIR and less in Red. Healthy vegetation has the larger absorption of the Red band, which is the visible light in the electromagnetic spectrum, compared with NIR band. It is because the healthy vegetation contains chlorophyll. Therefore, with this contrast, NDVI makes use of this characteristic and calculate the vegetation index. Davenport and Nicholson (1993) stated that NDVI is the most common vegetation index used for measuring the greenery of the small-scale or large-scale region. The equation of NDVI specifies in the following:

$$NDVI = \frac{(NIR - Red)}{(NIR + Red)} \text{ ————— (e)}$$

Also, the procedure for generating the NDVI of the study area will be presented in *Figure 5.3*. For the NDVI of the study area, the yellow area indicates the higher NDVI while the blue area presents the lower NDVI.

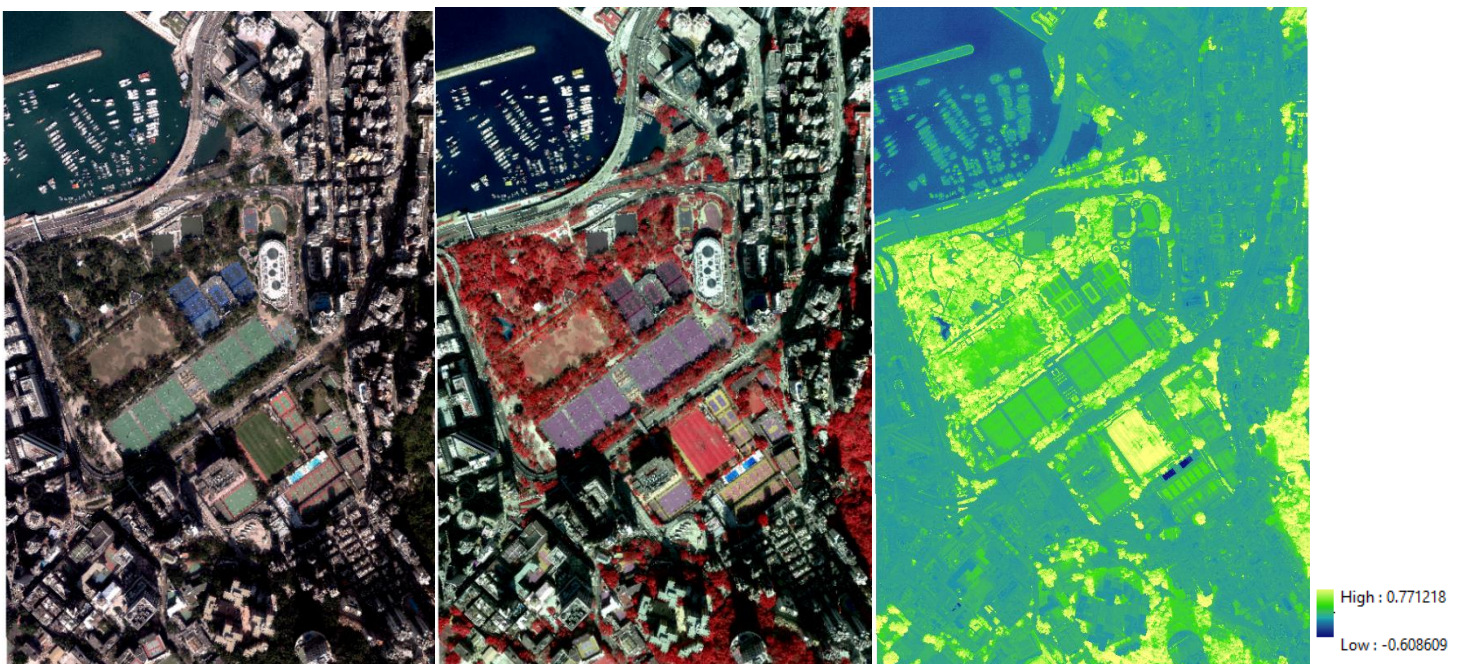


**Figure 5.3.** Original DAP (Left); False colour composites (Middle); NDVI (Right)

The range of NDVI is -1 to 1 and the large the value, the denser healthier vegetation. There is a simple classification when interpreting NDVI, where NDVI larger than 0 (i.e. positive value) represents the area covered by vegetation and NDVI smaller than 0 (i.e. negative value) represents area is not covered by vegetation (Gong, Lau, & Ng, 2016). The non-vegetated area can be water bodies, rock, built-up area, clouds etc. Also, there is a fine classification for NDVI. The value ranges from -1.0 to 0.0 indicates water bodies. Value ranges from 0.0 to 0.1 represent barren areas of rock, sand or snow. The value above 0.1 but lower than

0.3 indicates lower density vegetation, such as shrub and grassland and the value between 0.3 to 1.0 means dense vegetation, such as rainforest (Gong, Lau, & Ng, 2016).

### 5.4.1.2 Thresholding

This study used the NDVI of the study area for tree health detection in further processing and the details will be discussed in *Section 5.4.2*. The vegetation index can contribute to the extraction of vegetation area based on the specific NDVI value. For the particular NDVI value, including -0.3 to 0.0 and 0.0 to 0.1, these two classes of NDVI indicates the non-vegetated area and not water bodies, such as built-up area and barren (Yuan & Bauer, 2007). Therefore, the NDVI threshold values should be at least larger than 0.1. Apart from the study conducted by Yuan and Bauer, another study figured out more precise NDVI threshold values for detecting vegetation. Based on Akbar et al. (2019), the NDVI range for shrub and grassland is 0.18 to 0.27, the NDVI range for sparse vegetation is 0.27 to 0.36, and the NDVI range for dense vegetation is 0.36 to 0.74. Given the tree crown needed to be monitored, the sparse vegetation and dense vegetation are the target classes, thus, in this study, the pixel-based thresholding analysis with NDVI threshold values larger than 0.27 will be adopted. The result of the thresholding is presented in *Figure 5.4*.

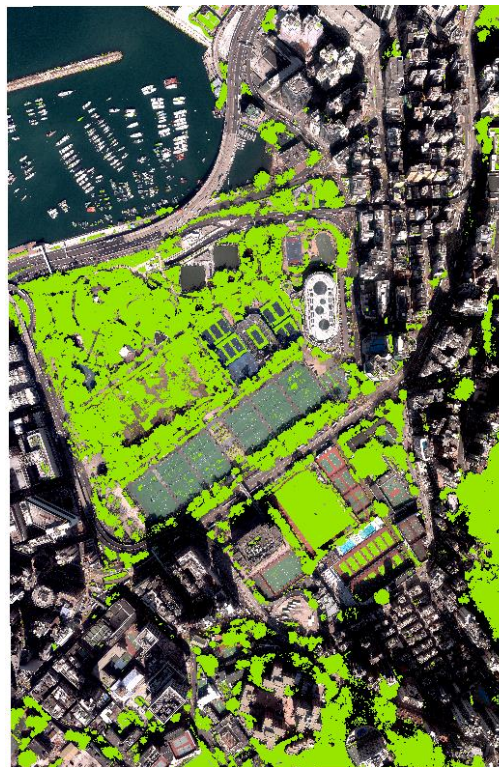


**Figure 5.4.** NDVI threshold value larger than 0.27 (Sparse and dense vegetation class)

*Figure 5.4* shows the NDVI index for the selected study area. No colour (NDVI less than 0.27) denotes areas with no vegetation, such as the area along the road, the building surrounding the Victoria Park, the sea located in the northern extent of the research field etc. Also, it found that Victoria Park has the largest amount of vegetation; therefore, its NDVI is comparably higher than that of the others.

Besides, *Figure 5.5* shows the effect of NDVI threshold values. For a low threshold value of 0.27, the

discretization that takes place in the playgrounds. Also, some of the tennis courts were considered as vegetation as the NDVI is larger than 0.27.

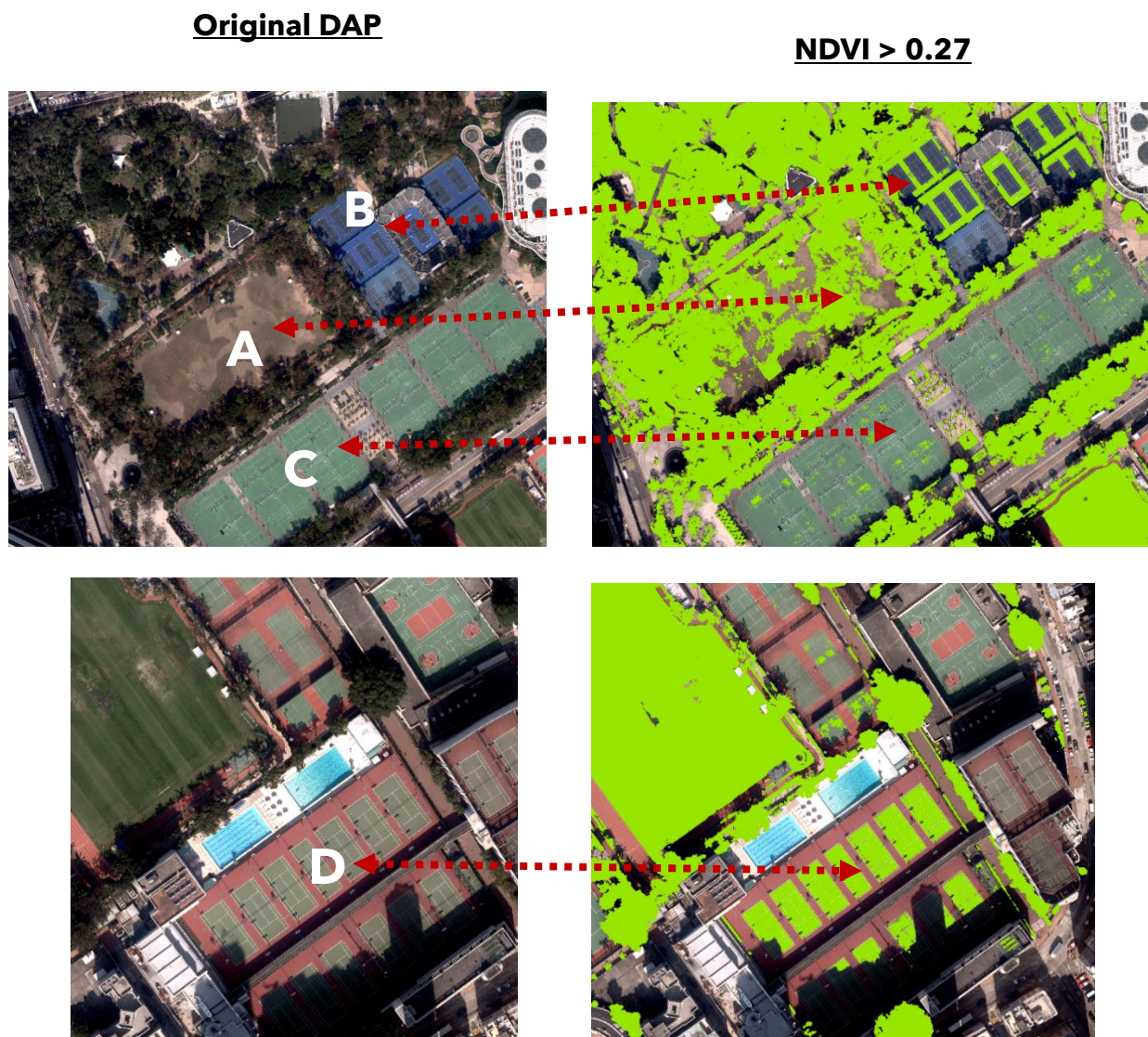


**Figure 5.5.** Non-vegetation land covers with NDVI > 0.27

In this regard, visual inspection for removing the non-vegetation manually is essential. As mentioned above, some non-vegetation land covers with NDVI larger than 0.27, while those land covers will not be mapped and focused on this study. Thus, after converting raster to polygon, the polygon of the non-vegetation area will be deleted, and *Figure 5.6* presents the optimized result of thresholding for vegetation extraction.

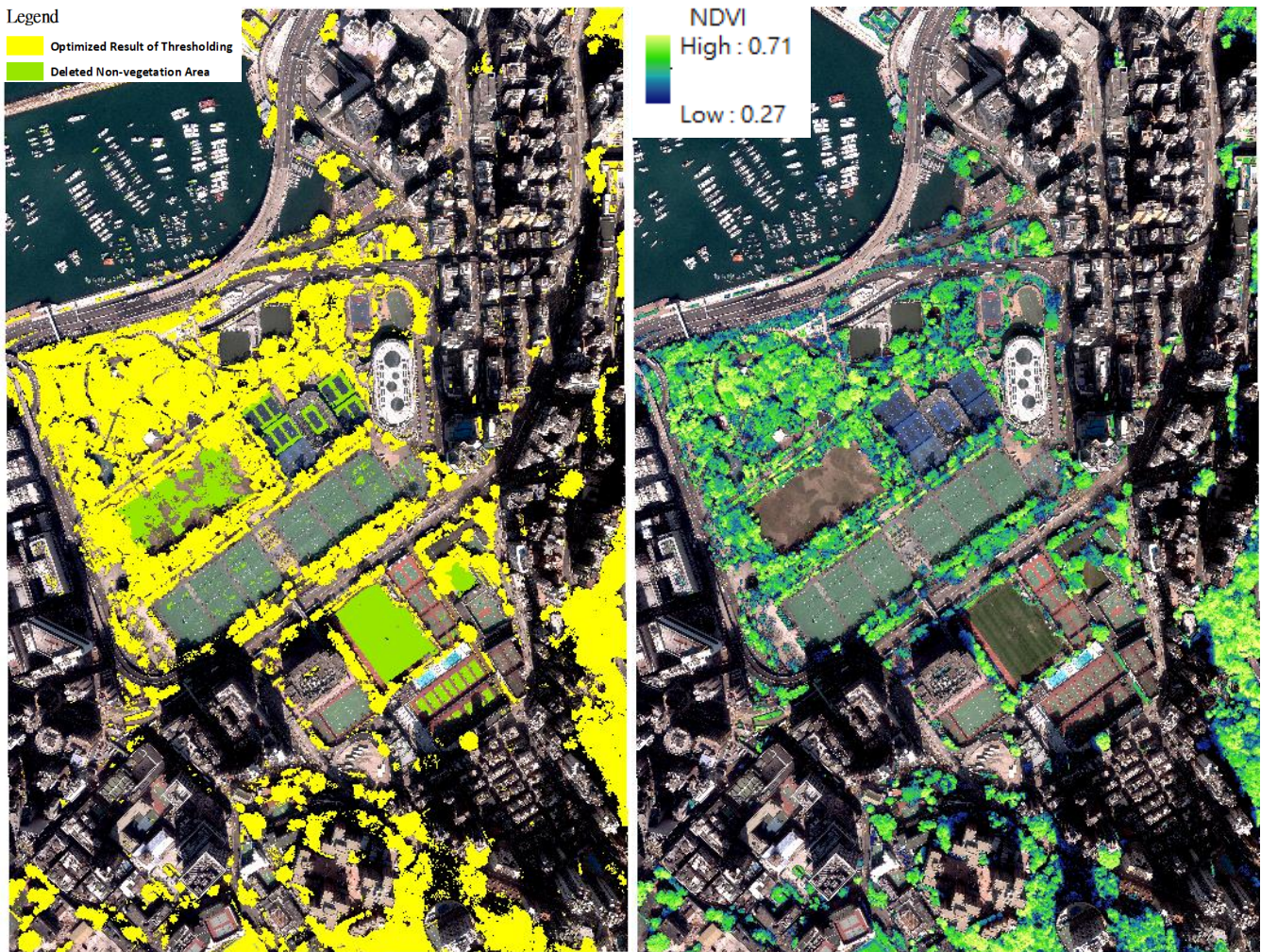


Figure 5.6. Optimized result of thresholding (Left) and NDVI of the delimited area of tree crown (Right)

### 5.4.2 Healthy Tree Crown Detection

Leaf cells scatter solar radiation in the near-infrared spectral region, which carries half of all incident solar energy. The energy level of each photon in the domain is not enough to synthesize organic molecules and the strong absorption of NIR only causes plants to overheat and may damage tissues. Therefore, green living plants that are darker in the Red band also appeared brighter in NIR (Gates, 1980). Since there is a significant difference between the two bands, scientists used the strong contrast in plant reflectance to determine these images' spatial distribution and the tree health status. NDVI is only a normalized difference and it only carries a small part of the information available in the original spectral reflectance data. Also, NDVI is sensitive to many interference factors. Therefore, it is usually only used for qualitative estimation. For each spectral band, the spectral reflectance is the ratio of reflected light to incident radiation, so it takes a value between 0.0 and 1.0. Moreover, according to the design, NDVI itself varies from -1.0 to +1.0. According to experience, the NDVI of densely vegetated canopy areas tends to be positive (0.3 to 0.8), while the principle of the unhealthy tree is characterized by lower positive values of this index (Putsay & Csiszár, 1997). For the healthy tree crown detection, NDVI will be adopted and more details, especially the threshold value for classifying the healthy and unhealthy leaves, will be discussed in the following section.

### 5.4.2.1 Index for Thresholding of Healthy Leaves

The spectral reflectance of vegetation is totally different from the reflectance of background materials (such as water, soil, and road surfaces) (Goward & Huemmrich, 1992). The vegetation absorbs light for photosynthesis. In the near-infrared region, vegetation has high reflectivity, and transitions to low levels very quickly between the red and near-infrared regions at about 750 nm (Daughtry, Walthal, Kim, De Colstoun & McMurtrey, 2000). This unique feature of the vegetation spectrum makes it possible to use Remote Sensing multispectral data to separate vegetation from background materials, which includes at least NIR and red zone reflections. Vegetation Indexes (VIs) are usually used to evaluate vegetation based on NIR and vegetation in the red spectral region or red edge (Xie et al., 2018). A high value of VI indicates healthy vegetation, while a low value of VI indicates the vegetation has the following subsequent conditions: senescent, diseased, leaf damage, water-stressed or that areas are without vegetation. NDVI is the ratio of the reflectance difference between NIR and red to the sum of NIR and red reflectance. As compared to unhealthy vegetation, healthy vegetation has a higher NDVI value. NDVI is a good indicator to distinguish between healthy and unhealthy vegetation (Kinyanjui, 2011).

In general, healthy plants usually have higher reflectance in the near-infrared region than diseased and stressed plants, distinguishing the plant's health condition. NDVI is a digital indicator for vegetation and vegetation intensity analysis using Red and NIR of the electromagnetic spectrum. Normally, healthy vegetation will absorb most visible light and reflect most of the nearby infrared region. Damaged or rare vegetation reflects more light than visible light, and less than NIR (Aggarwal, 2004). In addition, each tree with different health status has different reflectivity on distinct regions of the electromagnetic spectrum. It can be seen from *Figure 5.7* that the reflectance of healthy trees at the end of the visible part of the electromagnetic spectrum exceeds the red end of the spectrum and varies significantly in the near-infrared wavelength range of 700 nm and higher. This can be used to distinguish between two types of vegetation easily.

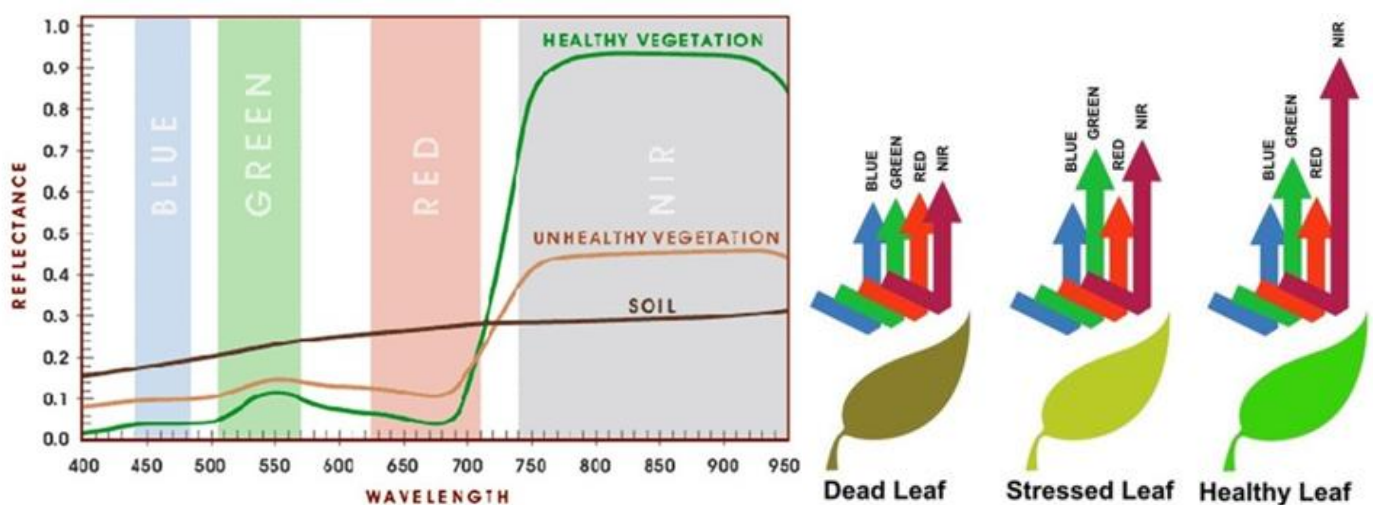


**Figure 5.7.** Difference of reflectance between the healthy and unhealthy vegetation (cited from Stoyanova, Kandilarov, Koutev, Nitcheva, & Dobrova, 2018)

To distinguish the healthy and unhealthy tree crown in the study area, the research threshold for unhealthy trees is 0.4 and 0.5. The minimum value, 0.4, was adopted for the large-scale implementation, thus, in this study, NDVI value of 0.4 will be applied for the pixel-based threshold to classify the healthy and unhealthy tree.

## 5.5 Result and Analysis

### 5.5.1 Classification of Tree Health Status

Based on the threshold of tree health conditions, basic tree health mapping can be generated. The raster-based map presented information at the pixel level, including tree health and vegetation indexes for each tree crown's pixel. Each tree was classified as either healthy or unhealthy. As mentioned above, NDVI with 0.4 is the threshold of classifying the healthy and unhealthy tree crown; therefore, the red colour represents the unhealthy tree crown, which has the NDVI lower than 0.4, while the green colour indicates the healthy tree crown, which has the NDVI larger than 0.4. *Figure 5.8* shows the basic classification of tree health.

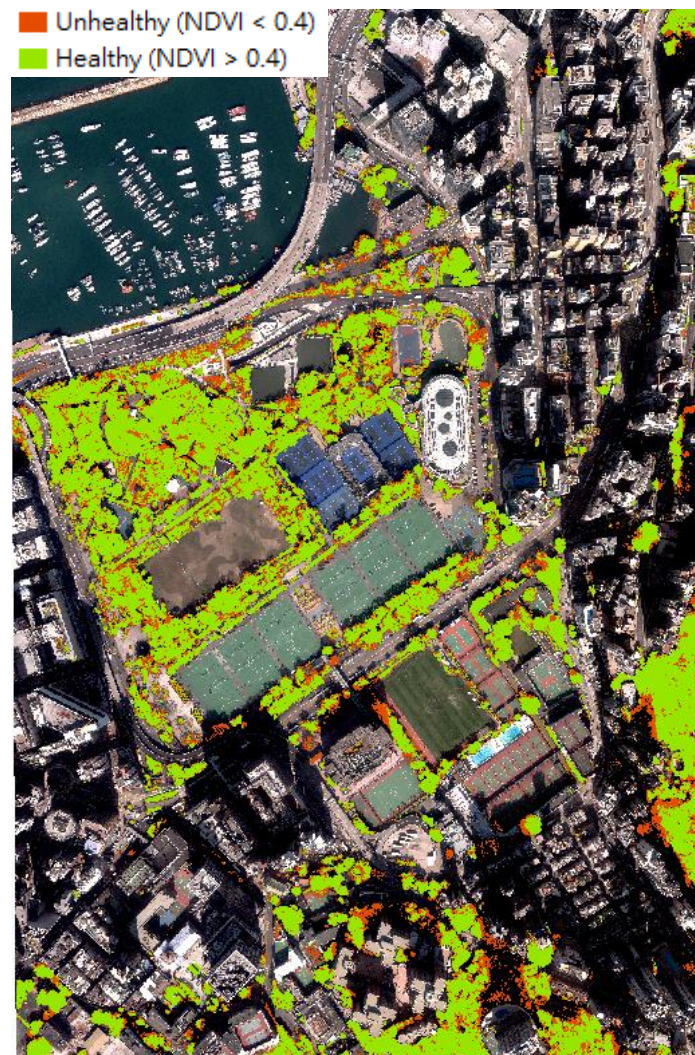


**Figure 5.8.** Basic classification of tree health condition

In general, it can be found that most of the area of unhealthy tree crown is out of the Victoria Park and the portion of the unhealthy area of each tree inside the Victoria Park is normally lower than that outside the Park. Also, the tree without healthy tree crown, which means that the whole tree crown is classified as unhealthy, cannot be found inside the Park but there are some located surrounding the Victoria Park as shown in *Figure 5.9*.

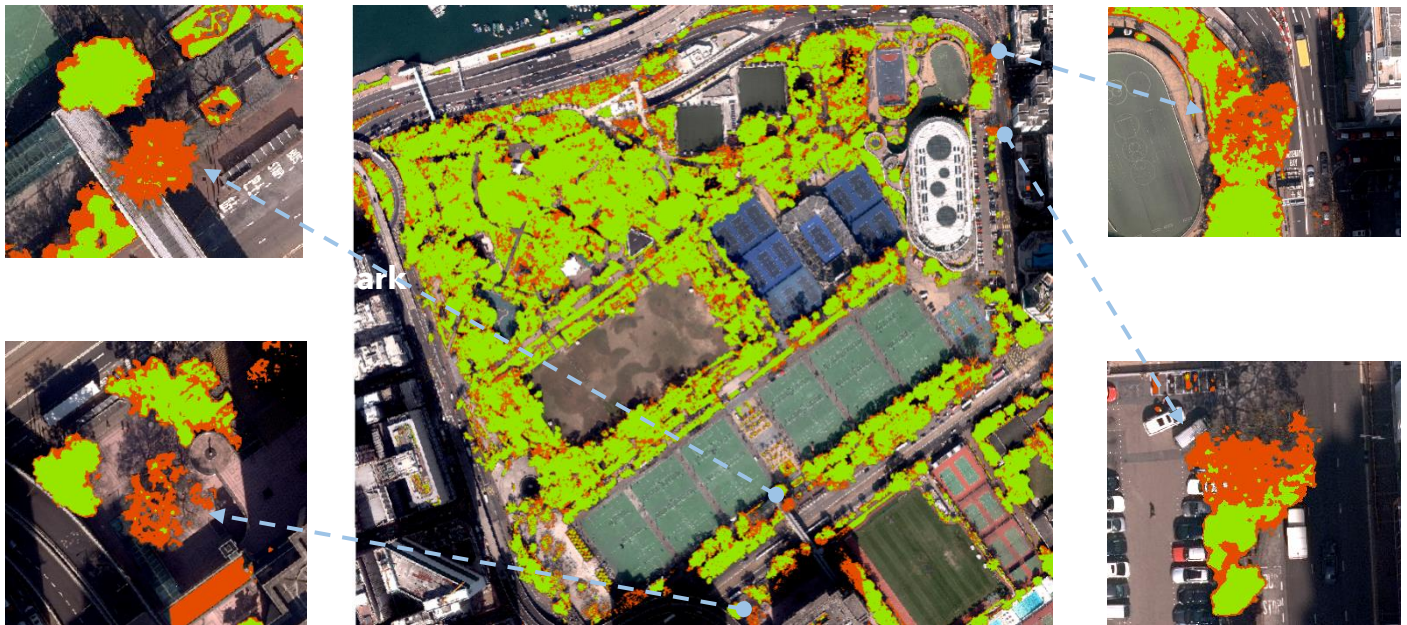


**Figure 5.9.** Location of the example of the tree with the significant large ratio of unhealthy tree crown

In order to present the comprehensive tree health condition of the study area, the colour ramp is used to show the scale of the health status of the part of healthy area of the tree crown. While the unhealthy area will be presented in red as indicated in *Figure 5.10*. The lighter green colour, the healthier the area of tree crown and vice versa. From *Figure 5.10*, the trees inside the Victoria Park typically have a healthier tree crown compared to the trees along the road as shown in *Figure 5.11* due to the larger ratio of dark green colour. Apart from Victoria Park, the group of trees in the southern part and southeastern part of the study area has a larger portion of healthy tree crowns than the unhealthy tree crown. While the standalone tree or the tree near the road typically have a lower portion of light green colour but a larger ratio of dark green, even the red colour (unhealthy), so the overall health condition of these trees is lower than that locating inside Victoria Park or the southern part.

The trees located in the Victoria Park also needed to be considered because most of the trees located inside Victoria Park are well-managed by the Leisure and Cultural Services Department (LCSD). With an area of over 19 hectares, Victoria Park is the largest park in Hong Kong Island, it provided adequate space for the growth of the tree. For example, there are 14 Old and Valuable Trees planted and many different species in Victoria Park, the ecological value of trees is very high. Besides, the Hong Kong Government aims to uplift the quality of the living environment in Hong Kong through active planting, proper maintenance and preservation of trees, and other vegetation. According to Greening, Landscape & Tree Management Section of Development Bureau (2016), the policy of the government is to provide priority protection to Old and Valuable Trees, Victoria Park has certain types of Old and Valuable Trees and many different tree species,

hence, it would be the government focus on managing the trees inside Victoria Park.

It is well known that the fundamental prerequisites for the vegetation growth are plenty of water and nutrient, however, roadside may not provide the basic needs for favorable vegetation growth due to the highly polluted, compact areas, and only suitable for the growth of a few tree species, which greatly affect their reachable tree age is lower than that of natural growth. On narrow pedestrian roads, trees are planted between pedestrians and roads, and the road usually narrow, which means there is not enough space for trees to grow, the roots of many trees are trapped in a small volume of soil, and the tree crown will be pruned artificially and this is easy to be observed that trees with narrow crowns and slender trunks.

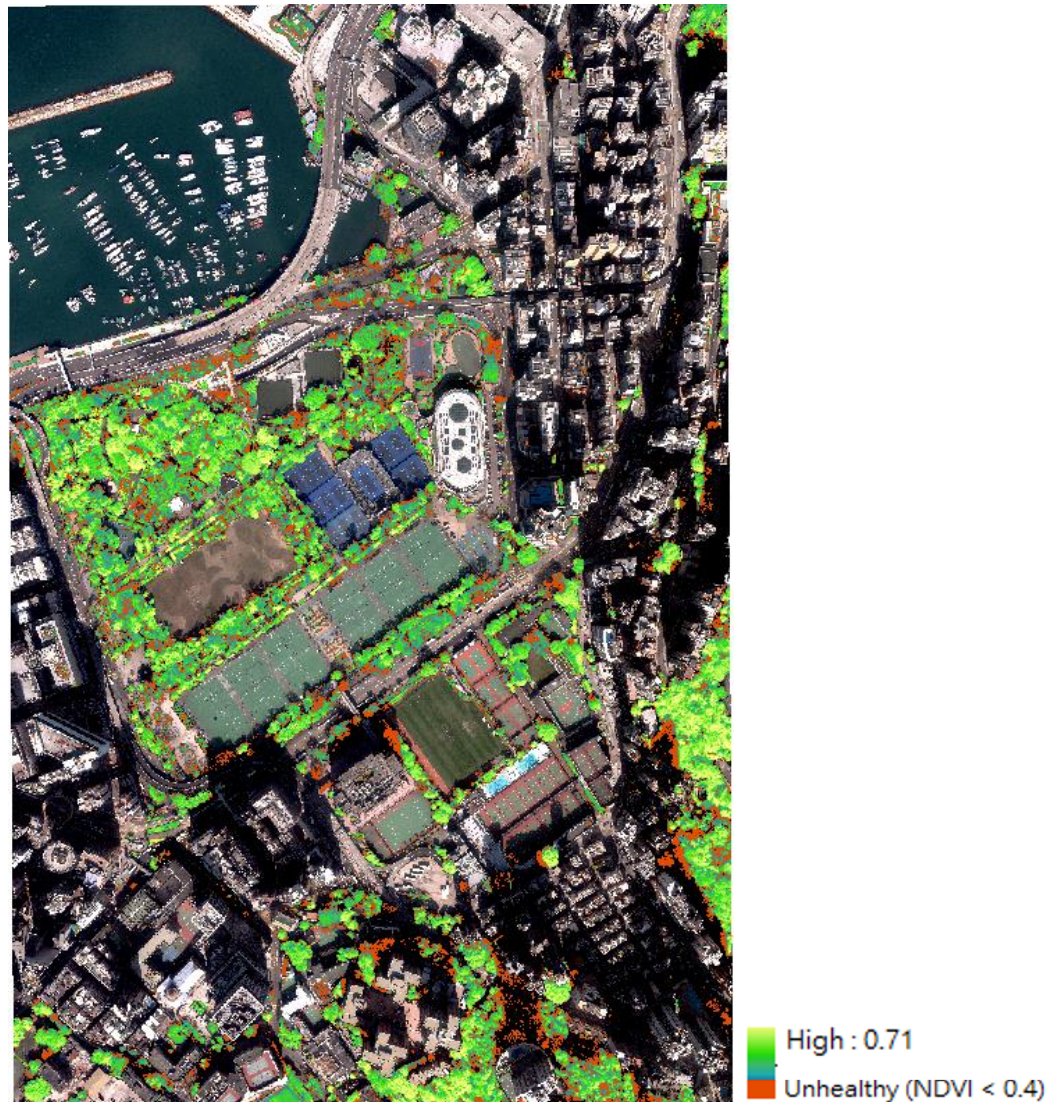


**Figure 5.10.** Tree health mapping of the study area

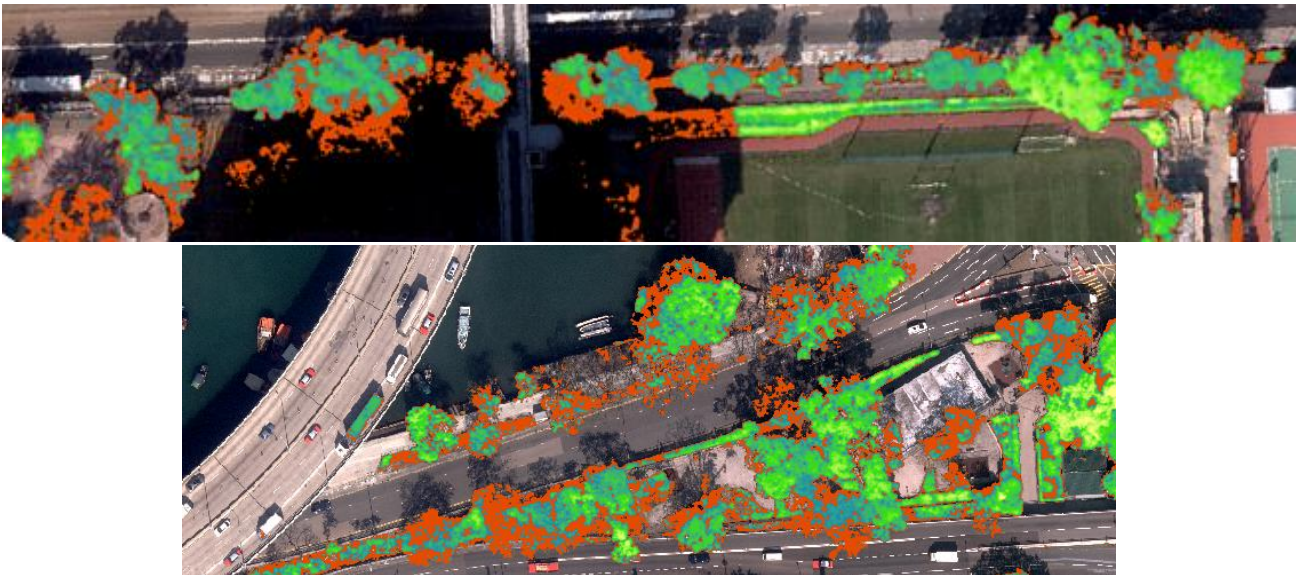


Figure 5.11. Tree health mapping of the roadside

The microscopic level will be discussed hereafter the macroscopic level presentation and analysis are shown in *Figure 5.8* to *Figure 5.11*. Six sample trees (STs) will be discussed for a detailed analysis of the tree health condition through area-based multispectral aerial imaging.

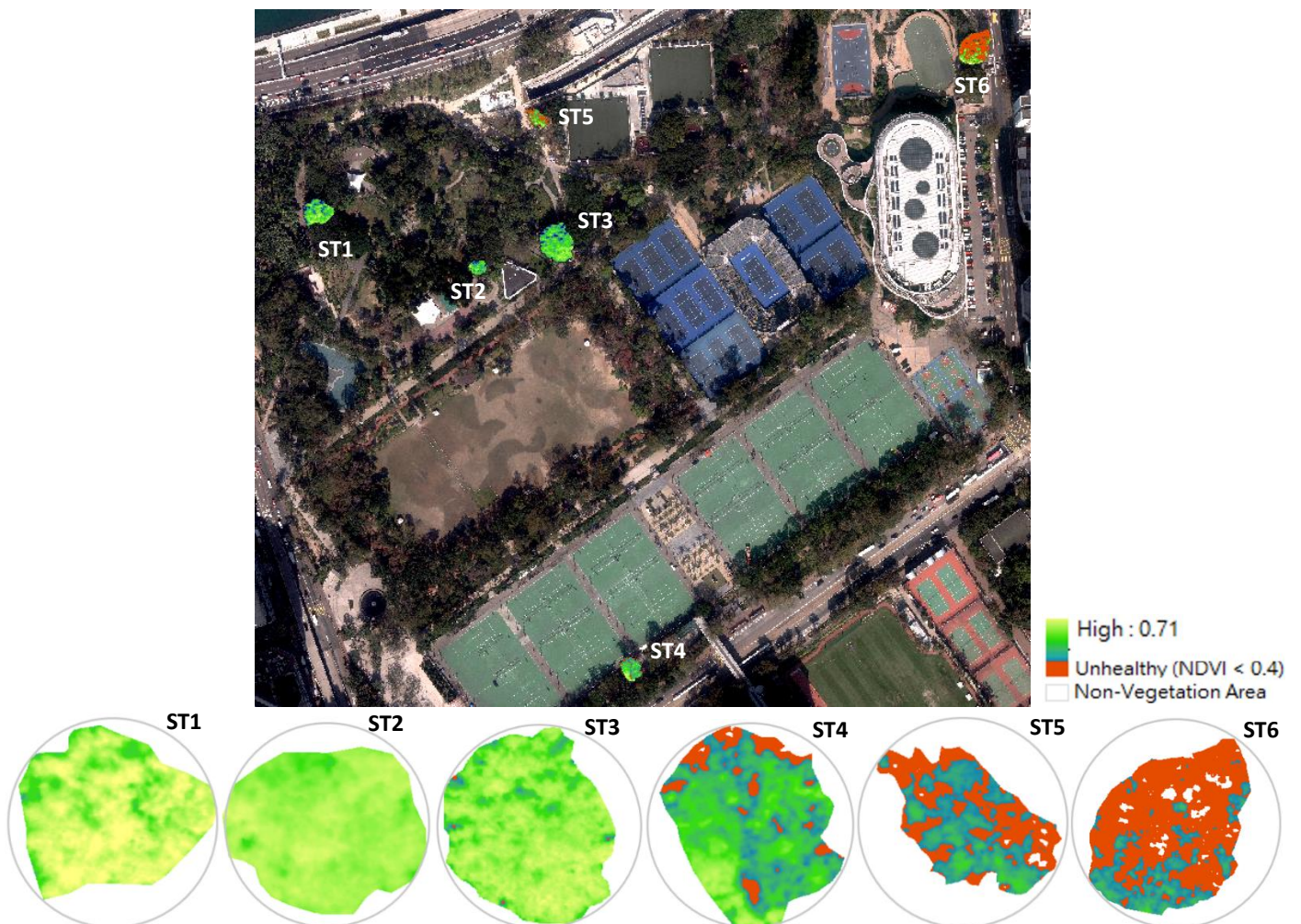


Figure 5.12. Location of the six sample trees and their detailed health condition

According to *Figure 5.12*, six STs are extracted and their detailed tree health condition can be investigated. Based on the ratio of the unhealthy tree crown area, the relative health status can be compared and hence to figure out which tree requires the immediate further inspection or maintenance. It can be found that the lighter the green colour, the healthier the tree crown, while the larger the area in red, the unhealthier the tree crown. ST1 has the largest area of light green colour and no unhealthy area, however, the ST6 has the largest area of unhealthy tree crown with the least light green colour. Accordingly, ST1 is the healthiest tree of all the STs. Apart from the qualitative analysis, the quantitative presentation will be discussed below for a comprehensive understanding of the tree health detection through multispectral aerial imaging.

Tree	Pixel Level				
	Pixels			Percentage (%)	
	Healthy	Unhealthy	Total	Healthy	Unhealthy
ST1	147740	0	147740	100	0
ST2	51933	0	51933	100	0
ST3	252328	395	252723	99.8	0.20
ST4	81876	10245	92121	88.9	11.1
ST5	33408	26648	60056	55.6	44.4
ST6	55591	142083	197674	28.1	71.9

**Table 5.2.** Quantitative presentation of the tree health condition of the six sample trees

In order to classify the tree health status of the specific tree, a self-defined standard can be adopted for better management. For instance, when the percentage of healthy tree crown is more than 70%, it can be classified as a healthy tree and those trees are deemed not require urgent or immediate maintenance while basic routine maintenance is still essential. When the healthy tree crown is between 50 to 70%, those trees can be classified as general and recorded with frequent maintenance. For the percentage of the healthy tree crown less than 50%, the unhealthy class is assigned, and an immediate inspection and maintenance is necessary to prevent the potential hazard. Therefore, in accordance with the aforementioned quantitative presentation, ST1, ST2, ST3, and ST4 are classified as having a healthy tree crown. ST5 is classified as general and ST6 is classified as having an unhealthy tree crown. After examining the tree species of ST5 and ST6, these two trees are deciduous, where the leaves fall in the winter season. The fallen leaves led to a reduction in NDVI, leading to a decrease of NDVI canopy conditions that were considered unhealthy. Therefore, the proposed Remote Sensing method can distinguish the abnormal tree crown conditions, either the unhealthy tree canopy or the change in leaves conditions. The canopy condition of the deciduous trees can be further examined in the spring or autumn seasons.

From the above analysis, tree health was mapped as either healthy or unhealthy at both the pixel and single tree levels. The trees near the parking lots and the road typically have a larger portion of unhealthy tree crowns than the trees inside the Victoria Park. In other words, these trees have a lower NDVI value compared to the trees planted in well-irrigated areas and there are quite photosynthetic activities in these trees that resulted in

a lower NDVI compared to the well-irrigated trees. By mapping tree health at these two different spatial scales, urban foresters can obtain critical tree management information. For example, individual tree-based data can be used to prioritize inspections to diagnose and tree health threats. At the area-based level, it is possible to identify the whole area's tree health condition to reflect the tree population's overall health.

## 5.6 Chapter Summary

This session demonstrated that multispectral aerial imaging could quantify vegetation in urban areas accurately, and tree detection in general was sensitive to the spatial resolution of data. By using multispectral and high spatial resolution Remote Sensing data, the health status of urban trees was evaluated. This urban tree detection method may be the most suitable for large-scale assessment, and it can provide valuable information for urban forester management. The tree health status map at the individual tree level can be used to determine the need for tree maintenance and replacement. Pixel-level patterns can provide information to determine whether pruning, irrigation or pest/disease treatment are needed. This tree health assessment method allows managers to identify unhealthy trees' locations for further diagnosis and treatment. It can track the spread of diseases and monitor seasonal or annual changes in tree health. Combined with the tree inventory, the data from this analysis can be used to budget the cost of tree processing and removal. In addition, it also provides tree health information, which is essential for modelling and analysis of environmental, social, and economic services produced from urban forests.

# CHAPTER 6 TREE HEALTH DETECTION THROUGH COMBINING THREE METHODS

## 6.1 Relationship of Health Condition between Tree Trunk and Tree Canopy

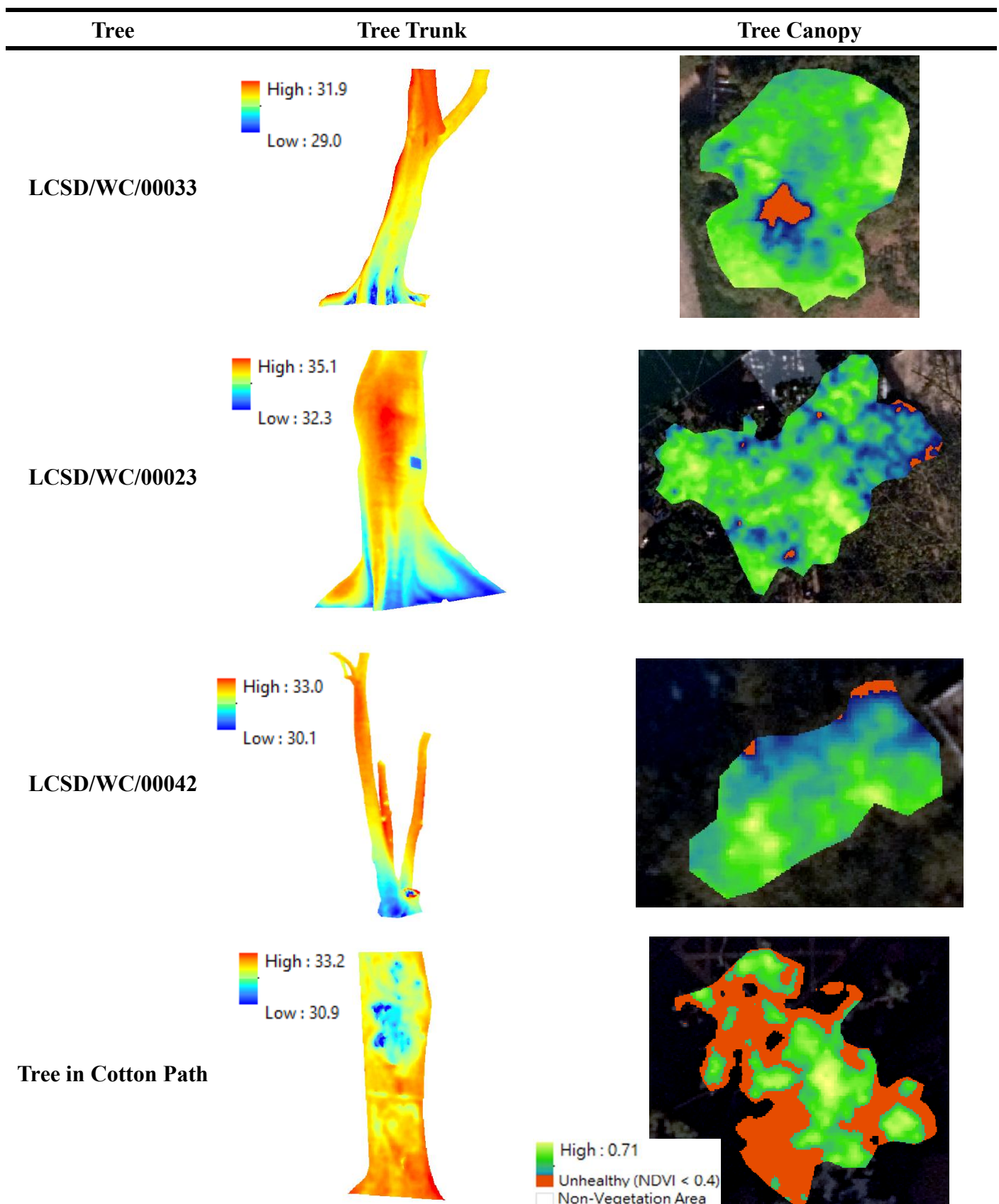


Figure 6.1. Health condition of tree trunk and tree canopy of the 4 sample trees

According to *Figure 6.1*, it can be found that there is no strong positive correlation between the health status of the tree trunk and tree canopy of a tree. For instance, the tree trunk of LCSD/WC/00033 and LCSD/WC/00023 are under healthy conditions, and their tree crown is also under healthy conditions. However, for the LCSD/WC/00042 and Tree in Cotton Path with a defect tree trunk, their tree crown can be healthy or unhealthy. Therefore, it is not possible to determine the health condition of a tree merely based on the health status of a tree trunk or tree crown but it is necessary to construct a system to monitor both tree trunk and tree canopy of a tree and hence to evaluate the overall health condition of a tree.

## **6.2 Result Consistency of the Health Condition of Tree Canopy Detected through Hyperspectral and Multispectral Imaging**

Typically, the result of tree health detection is the same as multispectral aerial imaging and hyperspectral imaging. As presented in *Figure 6.2*, the ST\_A and ST\_B have a healthy tree crown according to the result obtained from multispectral imaging, and they have the same result from hyperspectral imaging. Also, for another two unhealthy sample trees, they have the same result from hyperspectral and multispectral imaging. Therefore, there is a positive relationship between the two Remote Sensing technologies. To put it like this, the results of the health condition of tree canopy detected through hyperspectral and multispectral imaging are consistent.

However, the level of details of the result from hyperspectral imaging is higher than that of the multispectral imaging. Therefore, it is suggested that hyperspectral imaging should be applied to a tree-based project with a small amount of tree. For an area-based project with many trees required to be monitored, multispectral aerial imaging is undoubtedly more appropriate.

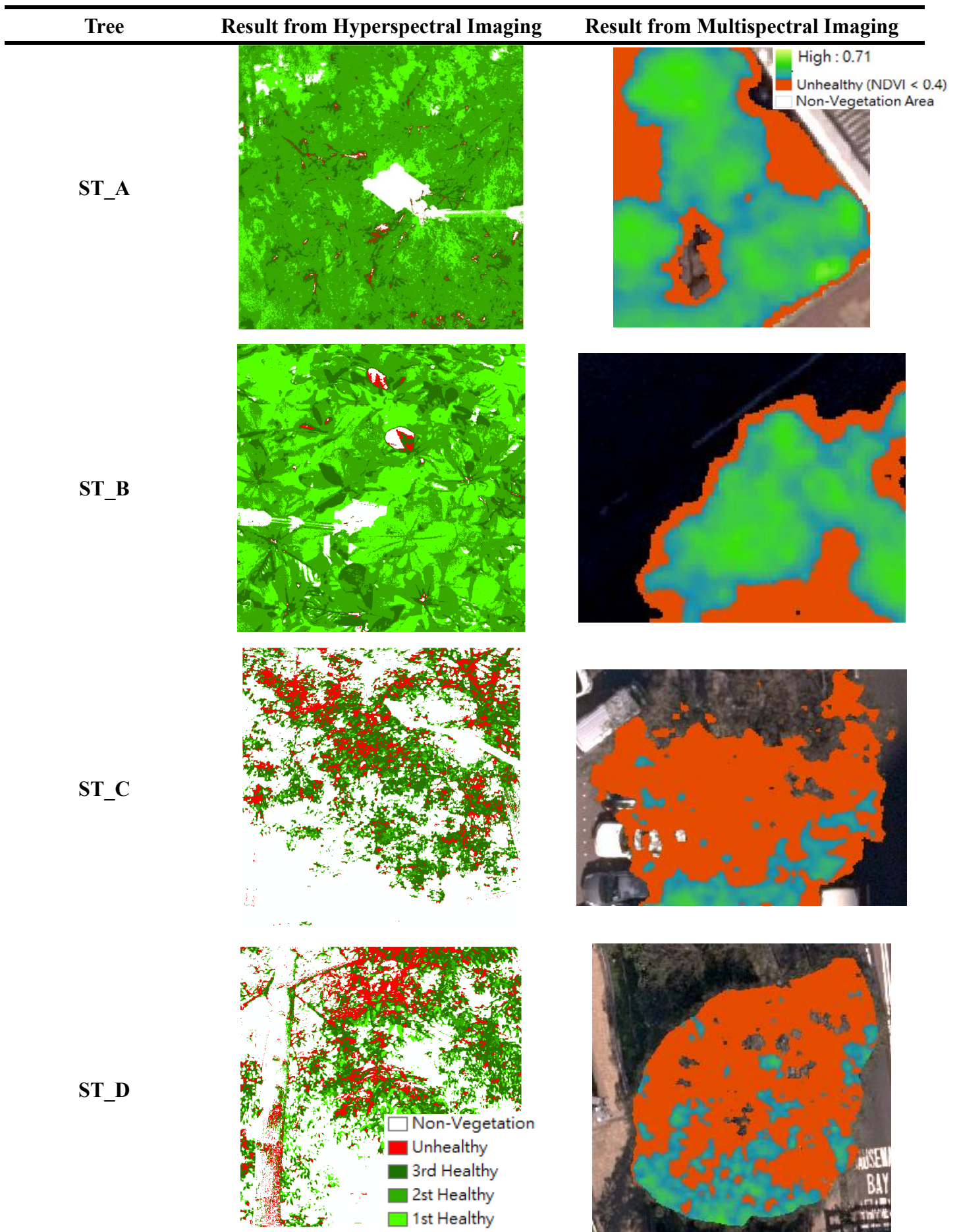


Figure 6.2. Health condition of tree canopy of the 4 sample trees from hyperspectral imaging and multispectral imaging

## CHAPTER 7 DISCUSSION AND RECOMMENDATION

---

In this session, it will mainly focus on discussing the pros and cons of the above technologies. The recommendation for these technologies will also be discussed.

To begin with, the advantage and the disadvantage of thermal infrared imaging will be discussed. IRT allows the trees to be viewed as a whole, which is advantageous to this technique, while the damage can be detected early even in trees with no external visual signs (Crisóstomo, Pereira, Roque, Jorge & Pitarma, 2018). IRT only requires very little time to perform the inspection and it is relatively easy to interpret the results. No contact with trees is required, and it can be safely observed within a distance of no more than 25 m (depending on the camera and lens). This is a safe technique for trees and inspectors as it does not emit radiation. IRT can also assess root damage in real-time and does not necessary to observe the higher part of the tree; hence, it is considered handy for the stability and safety evaluation (Catena, Lugaresi, Gasperoni, & Catena, 2002). IRT can easily monitor trees' health as it can follow up the determined pathological changes previously and new patterns that indicate the development of new pathologies (Catena et al., 2002). However, compared with other inspection methods, IRT's main advantage is distinguishable of functional tissues from dysfunctional tissues. In fact, IRT provides information to analyze trees' vitality and health in a non-destructive, fast and cost-effective manner (Catena & Catena, 2008). For the limitation, as with other non-invasive methods, the main limitation is that IRT cannot identify whether the detected damage is a void or tissue degradation, nor identify the cause to show an accurate indication on the degree of damage, despite IRT identifies damaged areas in the earlier stage and reduces the test time and damage progression.

Multispectral imaging has very detailed and strict band sets while hyperspectral images have many continuous bands. The advantages and disadvantages depend on the interest of users. Due to the small number of spectra, multispectral images are easier to use. This means the user can use multispectral images to distinguish the features, making more sense because it will narrow down the choices using frequency bands. However, the shadow effect would affect the result as the shadow will affect the NDVI, leading to misinterpretation in the tree health status for the tree health monitoring.

For the hyperspectral images, it can detect other features that cannot be detected by multispectral, which increases the possibility of new discoveries, that the specific features cannot be detected by using multispectral images and in turn hyperspectral imaging method can be considered. By monitoring the tree health condition, there are many vegetation indices, by utilizing the hyperspectral imaging method, in which more vegetation indices can be analyzed precisely rather than just using multispectral imaging. However, the hyperspectral imaging method still has some shortcomings. The main disadvantages are costly and complicated. Analyzing hyperspectral data requires fast computers, sensitive detectors and large data storage capabilities. Since the hyperspectral cube is a large multi-dimensional data set, which may exceed hundreds of megabytes, a large amount of data storage capacity is required. All these factors greatly increase the cost of acquiring and processing hyperspectral data. Similarly, one of the obstacles researchers have to face is to find ways to program hyperspectral satellites to classify the data by transmitting only important images, as transmitting and

storing large amounts of data can prove difficult and expensive.

All in all, the results of the above findings indicated that Remote Sensing methods have proven valuable to advance the field of vegetation monitoring. Remote Sensing offers a wide range, readily repeated measures of vegetation attributes and the possibility of 'lead' invisible indicators such as monitoring water stress in vegetation. Moreover, Remote Sensing is also particularly suited to change detection. Therefore, to manage and monitor the tree health condition, Remote Sensing technologies can be applied and highly recommended.

## CHAPTER 8 CONCLUSION

---

Urban trees and forests can provide a wide range of ecosystem services, such as cooling, air filtration, water interception, entertainment, etc., thereby greatly improving urban residents' quality of life. Meanwhile, due to various unhealthy factors, urban trees are under constant pressure. Due to human activities, air pollution is highly concentrated, and the soil is poorly contaminated in some locations such that their condition is varied. All these factors increase the threat of nutrients and water stress, which worsens the metabolism and growth of trees and reduces trees' ability to provide ecosystem services. Urban forests should be thoroughly managed, such as preventing, restoring, and maintaining urban trees, as serious tree health problems may weaken trees' stability and threaten public safety.

Remote Sensing is capable of providing vegetation health-relevant data. This project demonstrated three technologies about the procedures and the result of Thermal Infrared Imaging, Hyperspectral Imaging, and Multispectral Imaging, while comparison and recommendation were also made. Using these technologies demonstrates potential and promising methods to inspect the tree health problem; thus, the corresponding measures could be proposed to prevent damage and loss. Further application of Remote Sensing in tree monitoring is increasingly common nowadays; more research is required to use these techniques for a widespread application to maximize the technological capability in the various complex urban environment.

## REFERENCES

- Adam, E., Mutanga, O., & Rugege, D. (2010). Multispectral and hyperspectral remote sensing for identification and mapping of wetland vegetation: a review. *Wetlands Ecology and Management*, 18(3), 281-296.
- Aggarwal, S. (2004). Principles of remote sensing. *Satellite Remote Sensing and GIS Applications in Agricultural Meteorology*, 23-38.
- Akbar, T. A., Hassan, Q. K., Ishaq, S., Batool, M., Butt, H. J., & Jabbar, H. (2019). Investigative spatial distribution and modelling of existing and future urban land changes and its impact on urbanization and economy. *Remote Sensing*, 11(2), 105.
- Bellett-Travers, M., & Morris, S. (2010). The relationship between surface temperature and radial wood thickness of twelve trees harvested in Nottinghamshire. *Arboricultural Journal*, 33(1), 15-26.
- Boa, E. R. (2003). *An illustrated guide to the state of health of trees: Recognition and Interpretation of Symptoms and Damage*. Food & Agriculture Org.
- Calderón, R., Navas-Cortés, J. A., Lucena, C., & Zarco-Tejada, P. J. (2013). High-resolution airborne hyperspectral and thermal imagery for early detection of Verticillium wilt of olive using fluorescence, temperature and narrow-band spectral indices. *Remote Sensing of Environment*, 139, 231-245.
- Catena, G. (1993). Use of thermal scanner to diagnose tree cavities. *Rivista di Ingegneria Agraria (Italy)*.
- Catena, A. (2003). Thermography reveals hidden tree decay. *Arboricultural Journal*, 27(1), 27-42.
- Catena, A. (2003). Thermography shows damaged tissue and cavities present in trees. In *Nondestructive Characterization of Materials XI* (pp. 515-522). Springer, Berlin, Heidelberg.
- Catena, A., & Catena, G. (2008). Overview of thermal imaging for tree assessment. *Arboricultural Journal*, 30(4), 259-270.
- Catena, G., Lugaresi, D., Gasperoni, R., & Catena, A. (2002). Thermography reveals the occurrence of damage also in root system of trees. *Agricoltura Ricerca (Italy)*.
- Catena, G., Palla, L., & Catalano, M. (1990). Thermal infrared detection of cavities in trees. *European Journal of Forest Pathology*, 20(4), 201-210.
- Chilton, A. (2014). The Working Principle and Key Applications of Infrared Sensors. *Accessed*, 15, 2018.

- Crisóstomo, J., Pereira, C., Roque, E., Jorge, L., & Pitarma, R. (2018, November). Análise da salubridade de Árvores através da termografia por infravermelhos. In *Proceedings of the 1st Iberic Conference on Theoretical and Experimental Mechanics and Materials/11th National Congress on Experimental Mechanics* (pp. 4-7).
- Cumming, A. B., Galvin, M. F., Rabaglia, R. J., Cumming, J. R., & Twardus, D. B. (2001). Forest health monitoring protocol applied to roadside trees in Maryland. *Journal of Arboriculture*, 27(3), 126-138.
- Daughtry, C. S. T., Walthall, C. L., Kim, M. S., De Colstoun, E. B., & McMurtrey Iii, J. E. (2000). Estimating corn leaf chlorophyll concentration from leaf and canopy reflectance. *Remote Sensing of Environment*, 74(2), 229-239.
- Davenport, M. L., & Nicholson, S. E. (1993). On the relation between rainfall and the Normalized Difference Vegetation Index for diverse vegetation types in East Africa. *International Journal of Remote Sensing*, 14(12), 2369-2389.
- Degerickx, J., Roberts, D. A., McFadden, J. P., Hermy, M., & Somers, B. (2018). Urban tree health assessment using airborne hyperspectral and LiDAR imagery. *International Journal of Applied Earth Observation and Geoinformation*, 73, 26-38.
- Development Bureau. (2016). *Old and Valuable Trees in Hong Kong*. Retrieved from <https://www.greening.gov.hk/ovt/default.aspx>
- Derby, R. W., & Gates, D. M. (1966). The temperature of tree trunks—calculated and observed. *American Journal of Botany*, 53(6Part1), 580-587.
- Dutta, D., Singh, R., Chouhan, S., Bhunia, U., Paul, A., Jeyaram, A., & Murthy, Y. K. (2009, September). Assessment of vegetation health quality parameters using hyperspectral indices and decision tree classification. In *Proceedings of the ISRS Symposium, Nagpur, Maharashtra* (pp. 17-19).
- Erikson, M. (2004). Species classification of individually segmented tree crowns in high-resolution aerial images using radiometric and morphologic image measures. *Remote Sensing of Environment*, 91(3-4), 469-477.
- FLIR. (2020). FLIR T650sc. Retrieved from <https://www.flir.asia/products/t650sc/>
- Gamon, J. A., Penuelas, J., & Field, C. B. (1992). A narrow-waveband spectral index that tracks diurnal changes in photosynthetic efficiency. *Remote Sensing of Environment*, 41(1), 35-44.

- Gates, D. M. (1980). Evaporation and transpiration. In *Biophysical Ecology* (pp. 307-344). Springer, New York, NY.
- Gitelson, A., & Merzlyak, M. N. (1994). Quantitative estimation of chlorophyll-a using reflectance spectra: experiments with autumn chestnut and maple leaves. *Journal of Photochemistry and Photobiology B: Biology*, 22(3), 247-252.
- Gitelson, A. A., Merzlyak, M. N., & Chivkunova, O. B. (2001). Optical properties and nondestructive estimation of anthocyanin content in plant leaves. *Photochemistry and Photobiology*, 74(1), 38-45.
- Gitelson, A. A., Zur, Y., Chivkunova, O. B., & Merzlyak, M. N. (2002). Assessing Carotenoid Content in Plant Leaves with Reflectance Spectroscopy. *Photochemistry and Photobiology*, 75(3), 272-281.
- Gibson, P. J., & Power, C. H. (2000). *Introductory Remote Sensing: Principles and Concepts*. Psychology Press.
- Gong, F., Lau, K., & Ng, E. (2016, July). Exploring association between neighbourhood green space and physical activity of elderly in high density cities. In *Proceedings of the 36th International Conference on Passive and Low Energy Architecture, Los Angeles, CA, USA* (pp. 11-13).
- Govender, M., Chetty, K., & Bulcock, H. (2007). A review of hyperspectral remote sensing and its application in vegetation and water resource studies. *Water Sa*, 33(2).
- Goward, S. N., & Huemmrich, K. F. (1992). Vegetation canopy PAR absorptance and the normalized difference vegetation index: an assessment using the SAIL model. *Remote Sensing of Environment*, 39(2), 119-140.
- Greening, Landscape & Tree Management Section of Development Bureau. (2016). *Common Tree Problems*. Retrieved from [https://www.greening.gov.hk/en/tree\\_care/problems.html](https://www.greening.gov.hk/en/tree_care/problems.html)
- Hong Kong Observatory. (2018). *Super Typhoon Mangkhut (1822)*. Retrieved from <https://www.hko.gov.hk/tc/informtc/mangkhut18/report.htm>
- Huete, A., Didan, K., Miura, T., Rodriguez, E. P., Gao, X., & Ferreira, L. G. (2002). Overview of the radiometric and biophysical performance of the MODIS vegetation indices. *Remote Sensing of Environment*, 83(1-2), 195-213.
- Kinyanjui, M. J. (2011). NDVI-based vegetation monitoring in Mau forest complex, Kenya. *African Journal of Ecology*, 49(2), 165-174.
- Kornberg, H. (2020). *Metabolism*. Retrieved from <https://www.britannica.com/science/metabolism>

- Learning, D., SARscape, E. N. V. I., Data, E., & LiDAR, G. M. (2013). Vegetation analysis: using vegetation indices in ENVI.
- Lévesque, J., & King, D. J. (2003). Spatial analysis of radiometric fractions from high-resolution multispectral imagery for modelling individual tree crown and forest canopy structure and health. *Remote Sensing of Environment*, 84(4), 589-602.
- Liang, S., & Wang, J. (Eds.). (2019). *Advanced remote sensing: terrestrial information extraction and applications*. Academic Press.
- Maselli, F. (2004). Monitoring forest conditions in a protected Mediterranean coastal area by the analysis of multiyear NDVI data. *Remote Sensing of Environment*, 89(4), 423-433.
- Mattheck, C., & Breloer, H. (1994). Field guide for visual tree assessment (VTA). *Arboricultural Journal*, 18(1), 1-23.
- McAlpine, D. (1899). *Fungus diseases of citrus trees in Australia, and their treatment*. RS Brain, government printer.
- Meilleur, G. (2006). Basic tree risk assessment. *Arborist News*, 15(5), 12-17.
- Meola, C. (Ed.). (2012). *Infrared thermography recent advances and future trends*. Bentham Science Publishers.
- Mobasheri, M. R., Rezaei, Y., & Valadan Zoej, M. J. (2007). A method in extracting vegetation quality parameters using hyperion images, with application to precision farming. *World Appl. Sci. J*, 2(5), 476-483.
- HKSAR Press Releases. (2010). *LCQ17: Tree inspection*. Retrieved from <https://www.info.gov.hk/gia/general/201007/07/P201007070198.htm>
- North Carolina Climate Office. (2020). *The Water Cycle*. Retrieved from <https://climate.ncsu.edu/edu/WaterCycle>
- Nowak, D. J. (1994). Atmospheric carbon dioxide reduction by Chicago's urban forest. *Chicago's Urban Forest Ecosystem: Results of the Chicago Urban Forest Climate Project*, 83-94.
- Oliva, J., Thor, M., & Stenlid, J. (2010). Long-term effects of mechanized stump treatment against *Heterobasidion annosum* root rot in *Picea abies*. *Canadian Journal of Forest Research*, 40(6), 1020-1033.

- Perry, T. O. (1989). Tree roots: facts and fallacies. *Arnoldia*, 49(4), 3-29.
- Pettorelli, N. (2013). *The normalized difference vegetation index*. Oxford University Press.
- Pitarma, R., Crisóstomo, J., & Ferreira, M. E. (2019). Contribution to Trees Health Assessment Using Infrared Thermography. *Agriculture*, 9(8), 171.
- Potter, B. E., & Andresen, J. A. (2002). A finite-difference model of temperatures and heat flow within a tree stem. *Canadian Journal of Forest Research*, 32(3), 548-555.
- Primicerio, J., Gay, P., Ricauda Aimonino, D., Comba, L., Matese, A., & Di Gennaro, S. F. (2015). NDVI-based vigour maps production using automatic detection of vine rows in ultra-high resolution aerial images. In *Precision agriculture'15* (pp. 693-712). Wageningen Academic Publishers.
- Putsay, M., & Csiszár, I. (1997). Retrieval of surface reflectances from AVHRR visible and near-IR radiances. *Advances in Space Research*, 19(3), 523-526.
- Shanahan, D. F., Lin, B. B., Bush, R., Gaston, K. J., Dean, J. H., Barber, E., & Fuller, R. A. (2015). Toward improved public health outcomes from urban nature. *American Journal of Public Health*, 105(3), 470-477.
- Sims, D. A., & Gamon, J. A. (2002). Relationships between leaf pigment content and spectral reflectance across a wide range of species, leaf structures and developmental stages. *Remote Sensing of Environment*, 81(2-3), 337-354.
- SPECIM, SPECTRAL IMAGING LTD. (2020). *Specim IQ Technical Specifications*. Retrieved from <https://www.specim.fi/iq/tech-specs/>
- Stoyanova, M., Kandilarov, A., Koutev, V., Nitcheva, O., & Dobрева, P. (2018). Potential of multispectral imaging technology for assessment coniferous forests bitten by a bark beetle in Central Bulgaria. In *MATEC Web of Conferences* (Vol. 145, p. 01005). EDP Sciences.
- Survey and Mapping Office. (2018). *Digital Aerial Photo (DAP)*. Retrieved from [https://www.landsd.gov.hk/mapping/en/digital\\_map/service/product/dap.htm](https://www.landsd.gov.hk/mapping/en/digital_map/service/product/dap.htm)
- The Hong Kong Polytechnic University. (2018). *Smart Monitoring System for Urban Tree Management*. Retrieved from [https://www.polyu.edu.hk/ife/corp/en/publications/tech\\_front.php?tfid=18185](https://www.polyu.edu.hk/ife/corp/en/publications/tech_front.php?tfid=18185)
- Usamentiaga, R., Venegas, P., Guerediaga, J., Vega, L., Molleda, J., & Bulnes, F. G. (2014). Infrared thermography for temperature measurement and non-destructive testing. *Sensors*, 14(7), 12305-12348.

- University of Arkansas. (2020). *Common Forest Disease Problems*. Retrieved from <https://www.uaex.edu/environment-nature/forestry/health/disease-problems.aspx>
- USDA Forest Service. (2018). *Logging damage*. Retrieved from <https://www.forestryimages.org/browse/detail.cfm?imgnum=3036063>
- Vidal, D., & Pitarma, R. (2019). Infrared Thermography Applied to Tree Health Assessment: A Review. *Agriculture*, 9(7), 156.
- Weingartner, D. P., & Klos, E. J. (1975). Etiology and Symptomatology of Canker and Dieback Diseases. *Phytopathology*, 65, 105-110.
- Xiao, Q., & McPherson, E. G. (2002). Rainfall interception by Santa Monica's municipal urban forest. *Urban Ecosystems*, 6(4), 291-302.
- Xiao, Q., & McPherson, E. G. (2005). Tree health mapping with multispectral remote sensing data at UC Davis, California. *Urban Ecosystems*, 8(3-4), 349-361.
- Xiao, Q., Ustin, S. L., & McPherson, E. G. (2004). Using AVIRIS data and multiple-masking techniques to map urban forest tree species. *International Journal of Remote Sensing*, 25(24), 5637-5654.
- Xie, Q., Dash, J., Huang, W., Peng, D., Qin, Q., Mortimer, H., & Dong, Y. (2018). Vegetation indices combining the red and red-edge spectral information for leaf area index retrieval. *IEEE Journal of Selected Topics in Applied Earth Observations and Remote Sensing*, 11(5), 1482-1493.
- Yoshida, S., & Shirata, A. (1999). The mulberry anthracnose fungus, *Colletotrichum acutatum*, overwinters on a mulberry tree. *Japanese Journal of Phytopathology*, 65(3), 274-280.
- Yuan, F., & Bauer, M. E. (2007). Comparison of impervious surface area and normalized difference vegetation index as indicators of surface urban heat island effects in Landsat imagery. *Remote Sensing of environment*, 106(3), 375-386.